RIGA TECHNICAL UNIVERSITY

Faculty of Mechanical Engineering, Transport and Aeronautics

Institute of Mechanics and Mechanical Engineering

Milan Pravinbhai Dholakiya

The student of the Bachelor Study Programme "Engineering Technology, Mechanics and Mechanical Engineering"

(Student ID number: 171AMB116)

Numerical simulation of unidirectional composite materials damage under tensile loading.

Bachelor Thesis

Scientific advisor:

Dr. sc. ing., Prof. Olga Kononova

RIGA TECHNICAL UNIVERSITY

FACULTY OF MECHANICAL ENGINEERING, TRANSPORT AND AERONAUTICS

APPROVED

Director of Institute of Mechanics

			RTU, professor Vitālijs Beresņevičs			
	TA	ASK OF BACHELO	OR THESIS			
Field of study: Engineering Technology, Mechanics an			and Mechanical Engineering			
Stı	Student's name, surname: Milan Pravinbhai Dholakiya					
1.	under tensile loading	nerical simulation of un	idirectional composite materials damage			
3.	 The date of submitting the thesis is 10th of June 2020 Basic data on the tasks of Bachelor Thesis: FEM analysis is performed using solidworks software in order to analysis damage applied in composites. The content of the main part of the thesis: The main content of the thesis is as follows: 1) Introduction of composite materials; 2) Damages of composite materials; 3) Solidworks simulation for determining damage in the composite. 					
Supervisor:			/ Dr.sc.ing. Prof. Olga Kononova/			
		signature	name, surname			
Stu	ıdent	signature	/ Milan Pravinbhai Dholakiya/ name, surname			

Bachelor Thesis developed at RTU Institute of Mechanics	
Author of the thesis: Milan Pravinbhai Dholakiya	
(Sig	gnature, Date)
Scientific Advisor: Dr.sc.ing., Prof. Olga Kononova	
(Sig	gnature, Date)
Bachelor Thesis is suggested for defense:	
Head of the Department: Dr.sc.ing. Prof. Andrejs Krasnikovs	
(Si _§	gnature, Date)
Bachelor Thesis is defended at the meeting of	
the	
Secretary of commission	

ABSTRACT

The Bachelor thesis presents polymeric composite material, reinforced by glass fiber and its model damaged.

In this thesis, the FEM analysis using Solidworks software is performed for the damages in unidirectional composites under tensile loading.

The objective of the works is as follow: to study the damaged occurs in fiber and matrix and analyze the interaction between fiber and matrix during failure under tensile loading, as well to study how fiber volume fraction effects on fracture process.

The work contains of two parts: the theoretical part and the practical part. In the theoretical part are considered main types of damage in composites. The practical part includes the main aim of the work where 3D models of composites is created, and FEM analysis is performed in order to find the material behavior under tensile loading.

The following programs were used during the thesis: Solid works, Microsoft office Excel, Paint and Origin Pro.

Work contains Pages of text, Figures and references

Abstrakts (Abstract in Latvian)

Bakalaura darbā tika aplūkots polimeru kompozītmateriāls stiegrots ar stikla šķiedru un tas sabrukšanas modelis.

Darbā tika izpildīta GEM analīze, izmantojot programmu SolidWorks lai prognozētu vienvirziena kompozītmateriāla sabrukšanu stiepes gadījumā.

Daba galvenie mērķi ir: izpētīt sabrukšanu, kura notiek šķiedrās un matricā un izanalizēt iedarbību starp šķiedru un matricu sabrukšanas procesā stiepes slodzē, kā arī izpētīt kā armēšanas koeficients ietekmē sagrūšanas procesu.

Darbs sastāv no divām daļām: teorētiskā daļa un praktiskā daļa. Teorētiskajā daļā tika aplūkoti galveni sabrukšanas tipi kompozītmateriālos. Praktiskā daļa ietilpst darba galveno mērķi šeit aprakstīts kompozītmateriāla 3D modeļa izveidošana, kā arī GEM analīze ar mērķi noteikt materiāla uzvedību pie stiepes slodzes.

Darba tika izmantotas sekojošas programmas: Solid works, Microsoft office Excel, Paint and Origin Pro.

Darbs satur lpp, zīmējumu un literatūras avotu

TABLE OF CONTENT

1.	CO	MPOSITE MATERIALS	8		
	1.1.	HISTORY	8		
	1.2.	NEED OF COMPOSITE MATERIALS	9		
	1.3.	TYPES OF COMPOSITE MATERIALS	10		
	1.3.	.1. NATURAL COMPOSITES	11		
	1.3.	.2. USES OF NATURAL COMPOSITES	12		
	1.3.	.3. MAN-MADE COMPOSITE MATERIALS	12		
	1.4.	APPLICATIONS OF COMPOSITE MATERIALS	13		
	1.5.	TERMS RELATED TO COMPOSITE MATERIAL DESIGN	14		
2.	DA	MAGE OF COMPOSITE MATERIALS	16		
	2.1.	SOME PAST STUDIES	19		
	2.2.	DAMAGE OF FIBRES	20		
	2.2.	.1. Fibre characteristics	21		
	2.2.	.2. Fiber Failure Criterion	23		
	2.3.	DAMAGE OF MATRIX	25		
	2.3.	.3. Damage of Long Fibres and matrix	29		
,	2.4.	INTERLAMINAR DAMAGE (PROGRESSIVE FAILURE)	31		
3. Practical part30					
	3.1. F	Tiber Failure (Damage applying in fiber)	37		
	3.1.	.1 Structure of composites	38		
	3.1.	.2 Applying Boundary Condition	40		
	3.1.	.3 Results after simulation	41		
	3.2 M	Satrix Failure (Damage applying in matrix)	47		
	3.2.	.1 Structure of model 1	47		
	3.2.	.2. The structure of model 2	62		

3.3. Compare the results	69
Conclusions	70
Bibliography	71

1. COMPOSITE MATERIALS

When two or more constituent materials with significantly different physical or chemical properties are combined to produce a material that has different characteristics from the individual components, the material formed is known as composites, provided, the individual components are separate and distinct within the finished structure.[1] This differentiate the composites from mixtures and solid solutions.

A composite is a material that is formed by combining two or more materials to achieve some superior properties. [10]

Certain material can be classified as composite if [12]:

- 1. Combination of materials results in significant property changes.[12]
- 2. Content of the constituents is generally more than 10 %.
- 3. In general, property of one constituent is much greater (≥ 5) than the other [12]

1.1. HISTORY

- People have been making composites for many thousands of years. One early example is mud bricks. Mud can be dried out into a brick shape to give a building material. It is strong if you try to squash it (it has good compressive strength) but it breaks quite easily if you try to bend it (it has poor tensile strength). Straw seems very strong if you try to stretch it, but you can crumple it up easily. By mixing mud and straw together it is possible to make bricks that are resistant to both squeezing and tearing and make excellent building blocks. [14]
- Another ancient composite is concrete. Concrete is a mix of aggregate (small stones or gravel), cement and sand. It has good compressive strength (it resists squashing). In more recent times it has been found that adding metal rods or wires to the concrete can increase its tensile (bending) strength. Concrete containing such rods or wires is called reinforced concrete.[14]

Oldest application/existence application/existence of composite material

- 4000 B.C. laminated writing material from the papyrus plant
- 1300 B.C. Egyptians and Mesopotamian used straw bricks
- 1200 A.D. Mongols invented the first composite bow [13][12]

Composite Bow were used dates back to 3000 BC (Angara Dating). The Materials Used in composite bow were Wood, Horn, Sinew (Tendon), Leather, Bamboo and Antler (Deer horn). The Horn and Antler are naturally flexible and resilient, Sinews were obtained from back tendons or hamstrings of cows and deer, bladder of fish worked as glue and Sinew, Horse hair, Silk were used as strings.[12]

1.2. NEED OF COMPOSITE MATERIALS

Composite materials are needed because of their Enhanced desired properties such as: [12]

- Strength
- Stiffness
- Toughness
- Corrosion resistance
- Wear resistance
- Reduced weight
- Fatigue life
- Thermal/Electrical insulation and conductivity
- Acoustic insulation
- Energy dissipation
- Attractiveness, cost
- Tailorable properties

Along with these properties, Composites also possess High Fatigue Life, and High Specific Strength and Modulus.

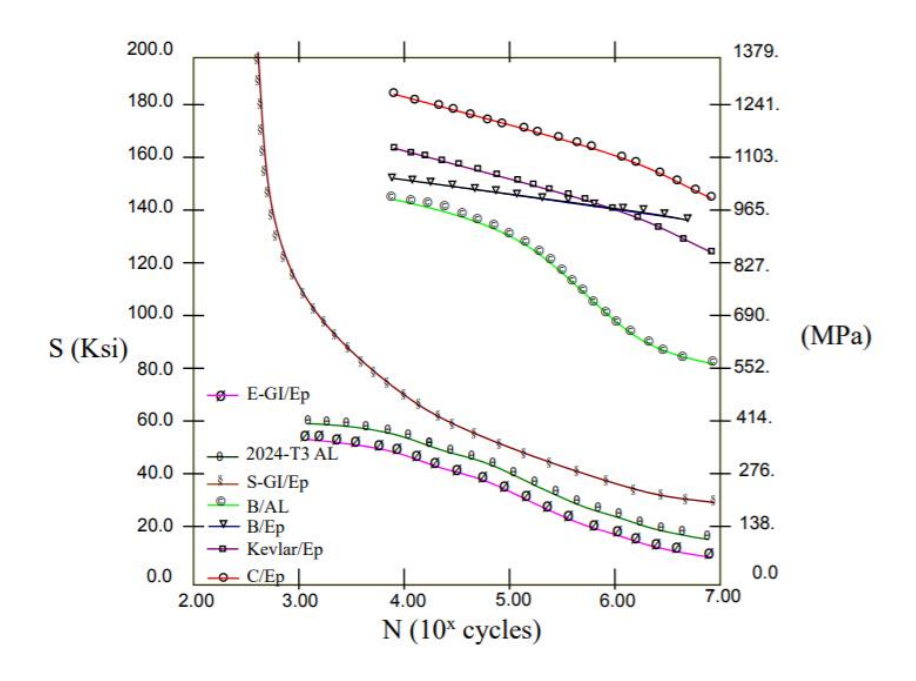


Fig 1.1. Graph showing High Fatigue Life of composites [53]

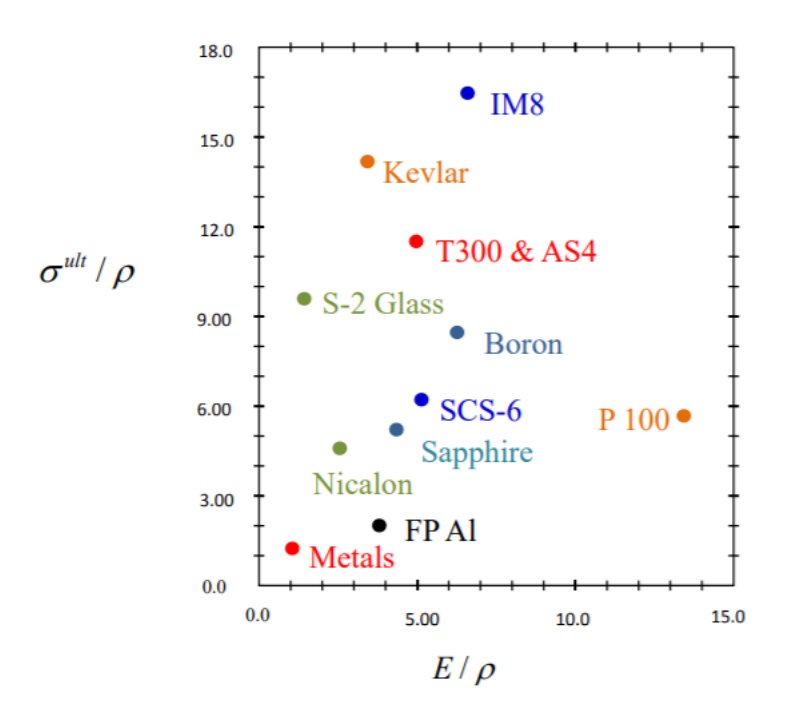


Fig 1.2. Graph showing High Specific Strength and Modulus [53]

1.3. TYPES OF COMPOSITE MATERIALS

1.3.1. NATURAL COMPOSITES

Almost all the materials which we see around us are composites. Some of them like woods, bones, stones, etc. are natural composites, as they are either grown in nature or developed by natural processes.[10] Natural composites generally show marked anisotropy - that is to say, their properties vary significantly when measured in different directions.[2]

Wood

Wood has cellulose fibers that are embedded in a compound called lignin. The function of cellulose fibers is to provide wood its ability to bend without breaking, while the lignin makes wood stiff.[2] Wood consist of thread-like hollow elongated organic cellulose which normally constitutes about 60-70% of wood of which approximately 30-40% is crystalline, insoluble in water, and the rest is amorphous and soluble in water. Cellulose fibres are flexible but possess high strength. The more closely packed cellulose, the higher density and higher strength fibre possess. The walls of these hollow elongated cells are the primary load-bearing components of trees and plants. When the trees and plants are live, the load acting on a particular portion (e.g., a branch) directly influences the growth of cellulose in the cell walls located there and thereby reinforces that part of the branch, which experiences more forces. [10]

Bone

Bone consist of collagen (a soft protein) (Currey 1983). and apatite (a strong but brittle mineral. The fibres usually grow and get oriented in the direction of load. Human and animal skeletons are the basic structural frameworks that support various types of static and dynamic loads. one special type of bone consisting of a flexible core and the hard enamel surface is tooth. The compressive strength of tooth varies through the thickness. The outer enamel is the strongest with ultimate compressive strength as high as 700MPa. Tooth seems to have piezoelectric properties i.e., reinforcing cells are formed with the application of pressure.[10]

The most remarkable features of woods and bones are that the low density, strong and stiff fibres are embedded in a low-density matrix resulting in a strong, stiff and lightweight composite. It is therefore no wonder that early development of aero-planes should make use of woods as one of the primary structural materials, and about two hundred million years ago, huge flying amphibians, Pteranodons and pterosaurs, with wing spans of 8-15 m, could soar from the mountains like the present-day hang-gliders. [10]

1.3.2. USES OF NATURAL COMPOSITES

- Woods, stones and clays formed the primary structural materials for building shelters.
- Natural fibres like straws from grass plants and fibrous leaves were used as roofing materials.
- Stone axes, daggers, spears with wooden handles, wooden bows, fishing nets woven with vegetable fibers, jewelleries and decorative articles made out of horns, bones, teeth, semiprecious stones, minerals, etc. [10]

The limitations experienced in using these materials led to search for better materials to obtain a more efficient material with better properties. This, in turn, laid the foundation for development of man-made composite materials.[10]

1.3.3. MAN-MADE COMPOSITE MATERIALS

The most striking example of an early man-made composite is the straw-reinforced clay which moulded the civilization since prehistoric times. Egyptians, several hundred years B.C., were known to reinforce the clay like deposits of the Nile Valley with grass plant fibres to make sun baked mud bricks that were used in making temple walls, tombs and houses. The watchtowers of the far western Great Wall of China were supposed to have been built with straw-reinforced bricks during the Han Dynasty (about 200 years B.C.). [10][31][32]

The twentieth century has noticed the birth and proliferation of a whole gamut of new materials that have further consolidated the foundation of modern composites. Numerous synthetic resins, metallic alloys and ceramic matrices with superior physical, thermal and mechanical properties have been developed. Fibres of very small diameter (<10µm) have been drawn from almost all materials. They are much stronger and stiffer than the same material in bulk form. The strength and stiffness properties have been found to increase dramatically, when whiskers (i.e., single crystal fibers) are grown from some of these materials. [10][32]

Composites, due to their heterogeneous composition, provide unlimited possibilities of deriving any characteristic material behaviour. This unique flexibility in design tailoring plus other attributes like ease of manufacturing, especially moulding to any shape with polymer composites, repairability, corrosion resistance, durability, adaptability, cost effectiveness, etc. have attracted the attention of many users in several engineering and other disciplines. Every industry is now vying with each other to make the best use of composites. [10][33]

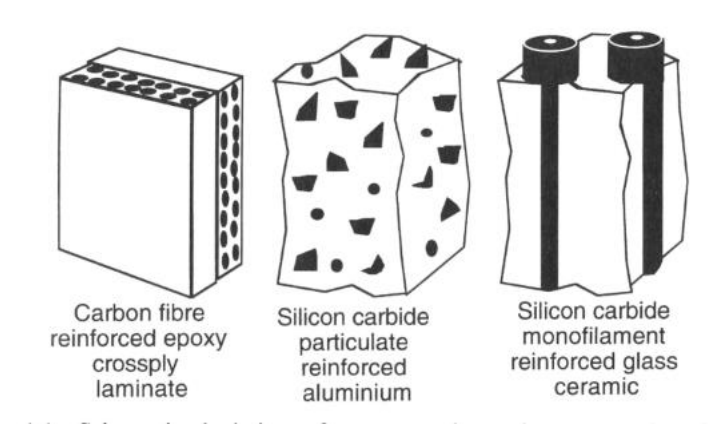


Fig 1.1. Schematic depiction of representative polymer, metal and ceramic matrix composites [10]

Composites make up a very broad and important class of engineering materials. World annual production is over 10 million tones and the market have in recent years been growing at 5-10% per annum. Composites are used in a wide variety of applications. Adaptation of manufactured composite structures for different engineering purposes requires input om several branches of science. [2]

1.4. APPLICATIONS OF COMPOSITE MATERIALS

- Composite materials are increasingly used in many industries including aerospace, automotive, electrical industries, etc. [1]
- Due to their significant advantages over metals, such as light weight, corrosion resistance, design flexibility, high strength, better fatigue life, etc. Composites also show an advantage over metal in low-temperature refrigeration systems [1] [2] and even in cryogenic environment.

- Strong, stiff and light composites are also very attractive materials for marine applications. GFRPs are being used for the last 3-4 decades to build canoes, yachts, speed boats and other workboats. [10]
- ship industries are also currently growing interest to use composites in a much larger scale. A new cabin construction material that is being tried in the Statendam-class ship building is a metallic honeycomb sandwich with resin-coated facing, that may lead to substantial weight saving. [2]
- The carbon/aluminium composite has been used for struts and foils of hydrofoils, and the silicon carbide/aluminium composite has been employed in pressure hulls and torpedo structures. The composites are also being increasingly used in the railway transportation systems to build lighter bogeys and compartments. [10]
- The other important area of application of composites is concerned with fabrication of energy related devices such as wind-mill rotor blades and flywheels.[10]
- The greatest advantage of using composite materials is their ability to be tailored to design requirements. The structure can be made stiffer in one direction and more flexible in another. This implies that the structure can be designed to be exactly as strong and stiff as it needs to be, leading to improved structural weight, aero elasticity and ultimately fuel efficiency. [35][36]

There are a few concerns which restrict the wider usage of composites: higher cost, complex fabrication, damage inspection, complex damage mechanism, etc. [2].

1.5. TERMS RELATED TO COMPOSITE MATERIAL DESIGN

Fracture: Conventionally, fracture is understood to be "breakage" of material, or at a more fundamental level, breakage of atomic bonds, manifesting itself in formation of internal surfaces. Examples of fracture in composites are fiber breakage, cracks in matrix, fiber/matrix debones, and separation of bonded plies (delamination). The field known as fracture mechanics deals with conditions for formation and enlargement of the surfaces of material separation. [7]

Damage: It refers to a collection of all the irreversible changes brought about in a material by a set of energy dissipating physical or chemical processes, resulting from the application of thermomechanical loadings. Damage may inherently be manifested by atomic bond breakage. Examples of damage in composites are multiple fiber-bridged matrix cracking in a unidirectional composite, multiple intralaminar cracking in a laminate, local delamination distributed in an interlaminar plane, and fiber/matrix interfacial slip associated with multiple matrix cracking.[7]

2. DAMAGE OF COMPOSITE MATERIALS

- Damage mechanisms in composites are not that well understood as that of metals.
 Defects can happen in composite materials and structures during the manufacturing process or in the service life of the structure/part/component. [17]
- The manufacturing process has a wide range of potential for causing defects in composites. The most common one is porosity which is the presence of a void in the matrix. The porosity can be caused by incorrect or non-optimal curing parameters [17]
- Inclusion of foreign bodies in matrix is another defect which happens during the manufacturing process which ranges from backing film to a greasy finger marks. In service defects in composite structures, mostly happens due to impact damages. [17]
- The most common defect due to the impact is delamination. In a laminated composite, delamination is separated layers, to form a mica-like structure with a significant loss in mechanical properties [18]. Delamination in curved composite beams under different static loadings has been investigated extensively by Khoshravan et al. [19].
- Matrix crack, fiber-matrix debonding, and fiber breakage also happen during the impact or other kind of severe loadings in composites [20] [21] [22].
- Other than impact, fatigue and lightning strikes can cause severe damages to composite structures and significantly reduce their mechanical properties. It is worth to mention that ply orientation of composite laminates has a significant role in stress concentration, fatigue life and mechanical properties of laminates [23] [24] [25] [26][5].

The growing usage of composite material in the structure of modern aircrafts has introduced new challenges. Aircrafts are vulnerable to the lightning strike that introduces direct and indirect effects in the skin of an aircraft. Damage development in a composite sample caused by flow of simulated lightning strike has been investigated by Gharghabi et al. [27] [28] . They have concluded that the flow of current impulse could induce irreversible damage and cause material property that might not be observable by simply inspecting the composite. This physical phenomenon has also, some practical implications that can be utilized in various high speed applications [29] .

There are a few stages of damage progression before ultimate failure. To discuss the progression of damage in composite materials, it is essential to consider the nature of the material. For instance, modern polymer composites that are based on glass, carbon, ceramic, or polymer fibers are anisotropic and heterogeneous. These materials have lower densities and possess high stiffness and strength in the direction of the fiber. This means that whenever there is an impact or stress applied along the direction of the fibers, these composites are generally strong and have reasonable impact resistance. In contrast, in the other direction the fibers tend to be weak and possess low impact resistance. Due to unexpected stresses along the weak directions of a fiber, damage can easily develop. As mentioned earlier, even though fiber fracture is the critical failure mode found in composite laminates, the damage is initiated in the form of matrix cracking or lamina splitting before progressing to delamination. This type of failure mode can be potentially dangerous as it can cause extensive subsurface delamination's which are not visible on the impacted surface. It has been found that delamination is the most severe type of damage since it significantly reduces the strength and stiffness of the structure. At each interface, delamination can occur in different sizes, shapes, and orientations. The delamination area size is usually measured using an ultrasonic C-scan, since this provides a projection of the entire damaged surface on a single plane. Note that in certain circumstances, depending on the type of material used and the damage extent, delamination cannot be measured using this ultrasonic C-scan technique and therefore microscopy images are needed to measure them.[6]

Composite is not atmospherically oxidised. Therefore, maintenance can be reduced. Atmospheric oxidation is the main reason for the maintenance of metal parts. Composites are much more susceptible to damage caused by heat and ultraviolet light than metal. Both heat and ultraviolet light can degrade the resin composite by initiating chemical reactions such as oxidation. Oxidation of the epoxy resin due to heat damage can reduce the physical properties and mechanical strength of a composite [4]. Severe degradation of the resin component may reduce the overall strength of the composites often leading to premature failure. Thermal pressure caused by lightning, engine overheating or engine fire has been observed to cause loss of mechanical strength, enbrittlement and finally cracking. When composites were introduced into aircraft components, unexpected damage from in-service conditions occurred. Most of the damage was categorised as internal defects and generally consisted of matrix cracking which was not easily detected on the surface of the specimen. This may have been due to impacts during flight operations, such as runway debris impacting on composite

airframes, bird-strikes during flight operations, or the dropping of hand tools during maintenance work. Under repeated or impact loads these materials were subjected to various forms of damage, mostly delamination and cracks [5]. In the laminated composites usually used in aircraft applications, damage can appear in various forms: matrix cracking, fibre fracture, fibre pull-out and delamination. These are all possible damage mechanisms which can be faced by composite laminates in the event of impact. When these materials are subjected to impacts, the structural integrity, stiffness and toughness of the material are significantly reduced, resulting in catastrophic failure of the structure in extreme scenarios. Impact damage can cause a reduction in the performance of composite structures.[3]

All structures are designed for a purpose. If the purpose is to carry loads, then a designer must assure that the structure has sufficient load-bearing capacity. If the structure is to function over a period of time, then it must be designed to meet its functionality over that period without losing its integrity. [35][36]

These are generic structural design issues irrespective of the material used. There are, however, significant differences in design procedures depending on whether the material used is a so-called monolithic material, e.g., a metal or a ceramic, or whether it is a composite material with distinctly different constituents. The heterogeneity of microstructure as well as the anisotropy of properties provide significantly different characteristics to composite materials in how they deform and fail when compared to metals or ceramics.[7]

The micromechanics of failure was developed to predict the failure of continuous fiber reinforced composites. A micromechanical approach using unit cells of square and hexagonal arrays was employed to compute the micro stresses of constituents and at the fiber—matrix interface, which were used to determine the failure initiation of a unidirectional ply. The constituent properties include two tensile and compressive strengths of fiber and matrix, plus normal and shear strengths at the interface. The matrix and interfacial dominated strength properties are determined by matching the micro stresses at the constituent levels with the observed transverse tensile and compressive strengths on the macro ply level. The longitudinal shear failure is then expected to be a result of damage progression after initial failure. Based on the current MMF, in the graphite/epoxy considered in this study both transverse tensile and compressive failure are expected to occur via matrix failure. However, in the glass/epoxy the transverse tensile and compressive failures are respectively caused by matrix failure and interfacial tensile failure. [11]

Due to the material and geometric inhomogeneity arising from the inclusion of fibers in the fiber reinforced composites, non-uniform micro-stresses at the constituent level develop by external mechanical and thermal loadings. Any point within the composite belongs to one of three regions, i.e., the fiber, the matrix, or the fiber–matrix interface. Ply failures initiate and can have dissimilar failure mechanisms depending on where the critical points exist. Therefore, appropriate failure criteria for each set should be used to judge where failure initiates [11]

2.1. SOME PAST STUDIES

As studied by Sato et al. (2019), interface failure and matrix failure are represented by cohesive zone modelling and continuum damage mechanics, respectively. A time-temperature superposition principle approach is applied in order to translate the difference in temperature as the difference in strain rate. The damage initiation depends on strain rate and temperature, while the cohesive zone modelling is assumed to be temperature- and time-independent. [45] Carrera et al. (2019) presented numerical results concerning the failure analysis of fiberreinforced composites. In particular, damage initiation and progressive failure are considered. The numerical framework is based on the CUF advanced structural models and the component-wise approach. Two approaches are assessed, including direct numerical simulations via micromechanical homogenization analysis and two-scale analysis. The results are compared with those from literature and attention is paid to the evaluation of the computational efficiency of the present numerical framework. In fact, 3D-like accuracy is sought with a reduced computational effort. [46] Qin et al. (2019) presented CEL models for 3D elements in PDMs of unidirectional composite structures and deduced their approximate formulae. The damage in unidirectional composite materials can be divided into fiber cracks and inter-fiber cracks. The fiber crack and inter-fiber crack directions are considered in the CEL derivations, and thus, the CELs of 3D elements that have various damage modes and damage directions could be obtained relatively precisely. [47] Koyanagi et al. (2014) studied the failure mode depends on the strain rate, with an interface-failure-dominant mode at a relatively high strain rate and a matrix-failure-dominant mode at relatively low strain rate. It aims to demonstrate this failure-mode transition by a periodic unit-cell simulation containing 20 fibers located randomly in the matrix. [48] **Koyanagi et al.** (2010) presented numerical simulation of a time-dependent interfacial failure accompanied by a fiber failure and examined their evolution under shear and compressive loads in single-fiber composites. The compressive load on the interface consists of Poisson's contraction for matrix resin subjected to longitudinal tensile load. As time progresses, compressive stress at the interface in the fiber radial direction relaxes under the constant longitudinal tensile strain condition for the specimen, directly causing the relaxation of the interface frictional stress. This relaxation facilitates the failure of the interface. [49] **Laš et al.** (2008) presented the numerical simulation of damage and fracture of unidirectional fiber-reinforced composite structures using the finite element method. The performance of the proposed model is demonstrated on examples of tensile tests of single-ply fiber-reinforced panels having different fiber orientations with and without stress concentrators. The numerical simulation is performed both as quasi-static and transient analysis and it involves identification and repetitive adjustment of material properties. [50]

2.2. DAMAGE OF FIBRES

Typical engineering composites consist of brittle fibres, such as glass or carbon, in a weak, brittle, plastic matrix such as epoxy or polyester resin. An important characteristic of these composites, however, is that they are surprisingly tough, largely as a result of their heterogeneous nature and the manner of their construction. During deformation, microstructural damage is widespread throughout the composite, but much damage can be sustained before load-bearing ability is impaired. Beyond some critical level of damage, failure may occur by the propagation of a crack which usually has a much more complex character than cracks in homogeneous materials. Crack growth is inhibited by the presence of interfaces both at the microstructural level between fibres and matrix and at the macroscopic level as planes of weakness between separate laminations in a multiple laminate. The fracturing of a composite therefore involves not only the breaking of the load-bearing fibres and the weak matrix, but a complex combination of excursions along these weak interfaces.

The microstructural inhomogeneity and the anisotropy of fibre composites are together responsible for the fact that the fracture of such materials is rarely a simple process. Although the complex combination of micro failure events that leads ultimately to destruction or at least to a deterioration of load-bearing ability can often give rise to surprisingly high levels of toughness, the same complexity makes it difficult, and sometimes impossible, to use procedures based on fracture mechanics for design purposes. There have been many theoretical and experimental studies of cracking in composites and of the mechanisms by which toughening is achieved, but there is still a large measure of disagreement about the contributions to the overall toughness of any given composite of the various processes by which cracks are stopped or hindered. The toughness of a composite is derived from many sources, and the relative magnitudes of the separate contributions will depend not only upon the characteristics of the separate components, but also on. the manner in which they are combined together. Carbon fibre reinforced resins, glass fibre reinforced thermoplastics, metal fibre reinforced metals, and steel or glass fibre reinforced cement all have their special characteristics. At the macroscopic level there are other discontinuities, the interfaces between laminae for example, or the resin-rich zones around the boundaries of fibre tows, and these discontinuities also affect crack growth. [9]

2.2.1. Fibre characteristics

Steel fibres used for reinforcing concrete, or the textile fibres such as Terylene, used to reinforce rubber tyres for motor vehicles, and Kevlar 49 reinforcement for brittle resins, may be classified as 'tough' because they are capable of considerable non-elastic deformation after yield. They show high tolerance of defects and surface damage, and it is unnecessary to resort to statistical methods to describe the failure of bundles (e.g. ropes). A bundle of such fibres possesses a large fracture energy, and a substantial proportion of this fracture energy can be transferred into a composite containing the bundle.[9]

By contrast, fibres such as glass, carbon, and boron, which have extremely high breaking strengths and elastic failure strains in the undamaged state, have very low fracture energies, of the order of only 10-100 J m-2, and their failure is governed by the nature of the flaw

distributions. The fracture energies of such fibres do not make any direct useful contribution to the failure energy of a composite.[9]

In a special category are the duplex fibre elements conceived and modelled by Morley. One kind of element consist of a strong but brittle sheath containing a coiled inner spring. This element confers high strength and rigidity on account of the sheath, and in unravelling the inner element a large amount of post-cracking fracture energy must be expended to withdraw the inner spring from the sheath. In some ways this mechanism relates to the true fibre pull-out effects observed in many fractured composites, and it also has a certain similarity with the manner in which the 'filament wound' secondary layer of a softwood cell wall 'unravels' during tensile failure of the tracheid. Failure of Scots Pine wood cell as result of fatigue is shown in fig 1.2 [9]

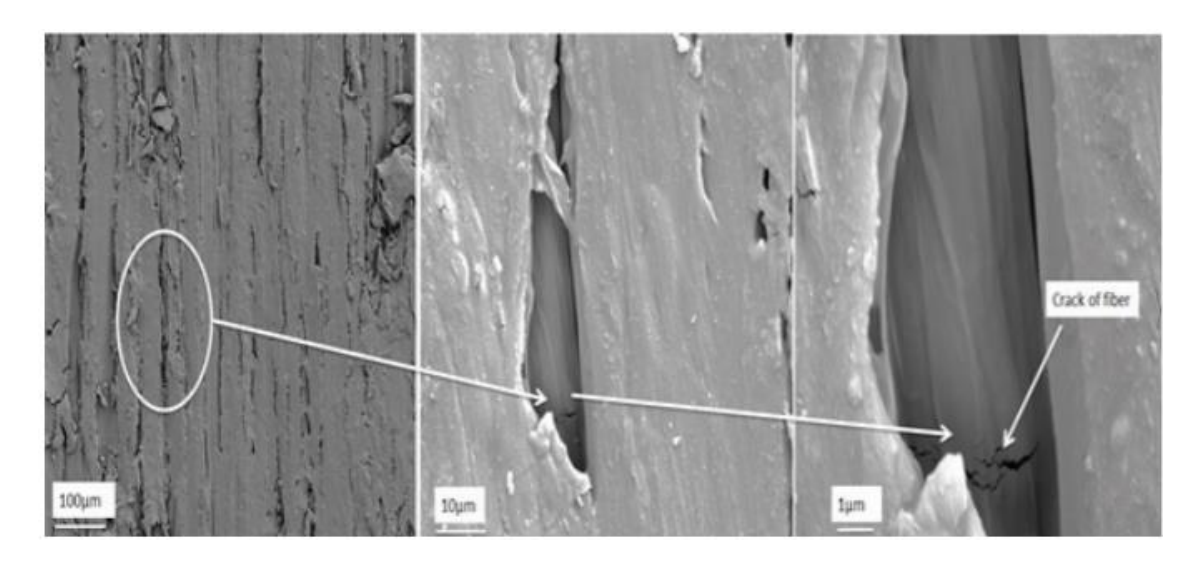


Fig 1.2. SEM image of longitudinal-radial sections of Scots pine. [37]

If the matrix and fibres can be said to have toughness in respect of their post-yield plastic deformability, and provided they can be fashioned into a composite without impairing that deformability, the fracture energy of the composite can be predicted as a mixture-rule sum of the fracture energies of the separate components:

$$Rc = Rm (1 - Vr) + RrVr$$
 (1)

where the subscripts c, m, and f refer to composite, matrix, and fibres, respectively. Cooper and Kelly have shown, however, that since fibre failure is localized, the contribution to the

total fracture energy made by the matrix metal must be increasingly reduced as V_r increases because of a reduction in the volume of plastically deforming matrix material. This plastic constraint imposes a triaxiality which reduces the effective value of Rm , and Cooper and Kelly, Gerberich,14 and McGuire and Harris have attempted, with some success, to model this effect on Rm with reference to observed behaviour. In terms of the ultimate tensile strengths u(u), failure strains s(u), and the fibre diameter d, expressions by Cooper and Kelly for Rm and by Gerberich for Rr can be added together to obtain the total composite fracture work:

$$R_C = R_m + R_f \tag{2}$$

$$R_{C} = d(1 - V_{t})^{2} V_{f}^{-1} \sigma_{m}(u) \varepsilon_{m}(u) + 2 dV_{t} \sigma_{f}(u) \varepsilon_{f}(u)$$
(3)

The terms in d and Vr modify the plastic work terms (of form us) to take into account the localized nature of the plastic deformation. Both matrix and fibres are subject to large local deformation and debonding usually occurs in systems like Cu/W, Al/W, or Al/steel. This decohesion relaxes some of the triaxiality that would otherwise prevail at the interface. Failure to deboned would cause conditions approaching plane strain throughout the composite and failure surfaces have the appearance of a flat, brittle-looking fatigue failure rather than the pseudo plane-stress (higher toughness) tensile failure of the locally separated components.[9]

2.2.2. Fiber Failure Criterion

In general, reinforcing fibers are considered to be transversely isotropic, and the tensile and compressible strengths in the longitudinal direction are remarkably high relative to strengths in transverse directions. Rationally, a quadratic failure criterion incorporating first-order and second-order stress invariants is employed to evaluate the synthetic effect of multi-axial stresses. The quadratic failure criterion for fiber takes on a form similar to the Tsai–Wu failure criterion for ply, but it is three-dimensional, involving six stress components [15]

$$\sum_{i=1}^{6} \sum_{j=1}^{6} F_{ij} \sigma_i \sigma_j + \sum_{i=1}^{6} F_{ij} \sigma_i = 1$$
 (4)

where coefficients Fij and Fi can be determined and summarized as follows:

$$\begin{split} F_{11} &= \frac{1}{X_f X_f'} \quad , \quad F_{22} = F_{33} = \frac{1}{Y_f Y_f'} \\ F_{44} &= \frac{1}{S_{f4}^2} \quad , \quad F_{55} = F_{66} = \frac{1}{S_{f6}^2} \\ F_{1} &= \frac{1}{X_f} - \frac{1}{X_f'} \quad , \quad F_{2} = F_{3} = \frac{1}{Y_f} - \frac{1}{Y_f'} \\ F_{12} &= F_{21} = F_{13} = F_{31} = \frac{1}{2\sqrt{X_f X_f' Y_f Y_f'}} \quad , \quad F_{23} = F_{32} = -\frac{1}{2Y_f Y_f'} \end{split}$$

where X_f , X_f' , Y_f , Y_f' , Sf4, and Sf6 are longitudinal tensile, longitudinal compressive, transverse tensile, transverse compressive, transverse—transverse shear, and longitudinal shear strengths of the fiber, respectively. Here, the interactive terms are determined so that the quadratic failure criterion is expected to be equivalent to the generalized von Mises failure criterion when all stress components are zero except for two normal stress components. [15]

Fiber is longitudinally continuous and has a considerably higher modulus and strength than those of matrix, which indicates that fiber supports almost the entire longitudinal tensile load applied to a ply; this statement is also valid for compressive load without consideration of fiber buckling. [15]

On the other hand, since fibers are bonded together by matrix, matrix plays a similar role under transverse and shear loads as fiber does under longitudinal load, which means that the strengths of matrix are major factors in determining ply strengths under those circumstances. As a natural result, all terms regarding transverse and shear stresses can be temporarily eliminated from the fiber failure criterion. Additionally, the adoption of a quadratic failure criterion requires the transverse tensile and compressive strengths of fiber, which are difficult to measure through experiment, so simplification is needed albeit the quadratic form is preferred. [15]

Finally, the simplified fiber failure criterion becomes the maximum longitudinal stress failure criterion:

$$-X_f' < \sigma_x < X_f$$

Generally, fiber breakage under longitudinal tension or compression (no buckling) can be considered a brittle behaviour, and hence no material property degradation model is needed.[15]

2.3. DAMAGE OF MATRIX

The functions of a matrix are [12]-

- 1. Holds the fibres together
- 2. Protects the fibres from environment
- 3. Protects the fibres from abrasion (with each other)
- 4. Helps to maintain the distribution of fibres
- 5. Distributes the loads evenly between fibres
- 6. Enhances some of the properties of the resulting material and structural component (that fibre alone is not able to impart). These properties are such as: transverse strength of a lamina Impact resistance
- 7. Provides better finish to final product.

Inclusion of foreign bodies in matrix is another defect which happens during the manufacturing process which ranges from backing film to a greasy finger marks.[4]

Two types of matrix cracks are observed generally on a damaged structure: shear cracks and tensile cracks.

Tensile cracks are due to contact forces and are observed when the in-plane normal stresses exceed the transverse tensile strength; while for shear cracks the damage propagates at an angle from the mid-surface [25].

This indicates that transverse shear stresses play an important role in their formation. There are differences between matrix cracks occurring on thin and thick plates. For a thick plate, matrix cracking starts to propagate on the very first layer of the impacted surface and the damage progresses from the top downward, resulting in a pine-tree pattern. Conversely, for a thin plate the matrix cracking begins on the lowest layer and moves to upper layer due to bending stresses on the rear surface of the plate, leading to a reversed pine-tree pattern as illustrated in Fig. 1.2.[6]

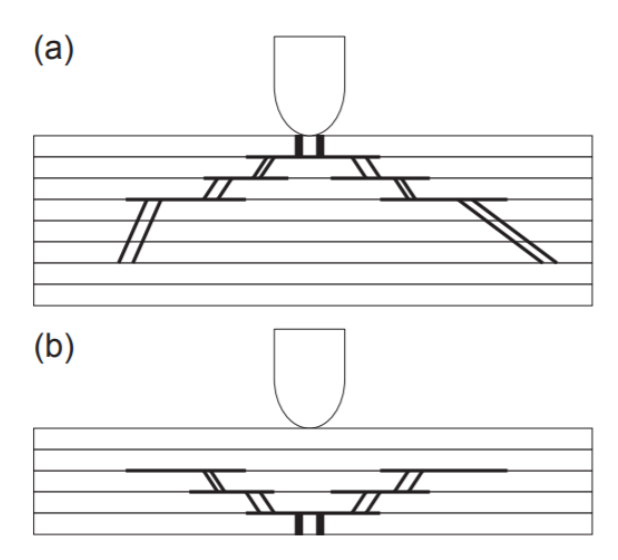


Fig. 1.2. Types of matrix cracks (a) Pine tree and (b) reversed pine tree damage patterns [38].

Metals such as aluminium or thermoplastics such as nylon, are tough matrixes with fracture energies of the order of 103 -105 J m - 2. They show extensive post-elastic deformation but have low yield points, and it may be impossible to propagate brittle cracks in them unless they are heavily cold-drawn, fatigued, or in thick sections. When reinforced with large volume fractions of hard, rigid, particulate matter, as in cermet's for example, the crack path may be substantially modified, sometimes passing through particles and sometimes through the matrix. The overall composite toughness is usually much lower than the inherent toughness of the matrix, partly because of the low fracture energy of the filler and partly because of the lower effective toughness of the plastically' constrained matrix between the filler particles. When ductile matrixes are reinforced with high-modulus high-strength low-ductility fibres (carbon or glass fibres in nylon, or boron fibres in aluminium are good examples) their toughness will usually be seriously impaired, particularly if the fibres are short or the volume fraction is low, because their intrinsic ability to sustain large plastic flow is reduced without a compensatory increase in modulus or strength. Brittle matrixes such as cement and thermoset resins have fracture energies of the order of only 100 J m-2. In most practical composites such as glass or carbon fibre 'reinforced plastics (GRP or CFRP) the volume fraction of reinforcement Vf is high, often greater than 0~50. A' crack therefore spends relatively little time propagating through large zones of pure matrix, and toughness contributions from the matrix itself can be ignored. In low Vf composites, however, such as steel fibre reinforced cement (FRC) where there may be only a few percent of fibres [9]

Matrix cracking may also be inhibited by the elastic constraint imposed on it by the presence of a rigid particle or fibre. In order for an increment of matrix crack growth to occur, a critical crack opening displacement (COD) at the crack tip must be exceeded. A stiff fibre, well bonded to the matrix, will locally increase the effective stiffness of the matrix at some distance from th,e fibre itself. The nearer the crack tip approaches the fibre, the greater is the apparent stiffness of the matrix and the higher the load that must be applied to the composite in order to achieve the critical COD. The magnitude of this effect will depend on the relative stiffness and fracture toughness of fibre and matrix. [8]

The model for these curves is a crack of some arbitrary initial size Co at an initial distance from the fibre of 50 fibre diameters (cement) or 200 diameters (glass/resin). As it extends towards fibre the effective composite V_f (and therefore stiffness) increases, as does the current level of stress intensity K where the applied stress level is assumed to remain constant. When the current increase in K (over the level remote from the fibre) equals the current increase in $(EG)^{1/2}$ the crack stops. The increase in $(EG)^{1/2}$ is simply the ratio $(Ec/Em)^{1/2}$, while the increase in K is $(C/C_0)^{1/2}$. This crude model suggests that a crack several mm long in a cement matrix will not be affected by a steel fibre until it has approached within about 5 fibre diameters, depending on the initial crack size, whereas a crack about 1 mm long in polyester resin will feel the effect of a glass fibre when it is still some 10 or more diameters away. [8]

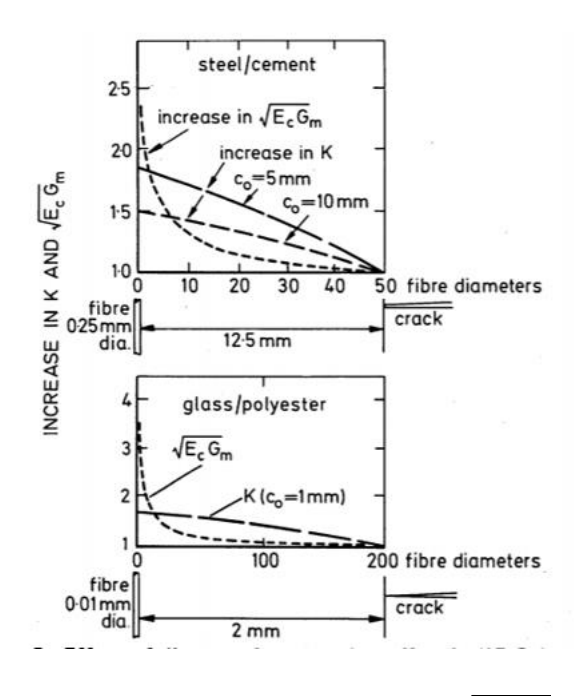


Fig. 1.3. effect of distance from K and $\sqrt{E_C G_m}$ [8]

The negative stress concentration in models of this kind arises because the fibres are more rigid than the matrix. The actual strength of the fibre, provided it is at least as high as that of the matrix, is irrelevant. Bowling and Groves have considered an extension of this treatment in which propagation of the crack tip through the matrix is hindered by unbroken fibres bridging the matrix crack behind the crack tip. For a double cantilever beam sample, they summed the bending moments, which were positive for the applied load and negative for the fibres in the tied zone, to obtain an effective crack tip stress intensity factor. As before, crack extension in the matrix is still governed by the ordinary matrix K1C value, but in the presence of a tied zone higher applied loads are required to satisfy the failure criterion K=K1C The fracture resistance of brittle matrixes may also depend on the speed of crack growth. The surface of a brittle resin cracked by a slowly growing crack is usually much rougher than the mirror finishes of a rapidly cracked surface, and the corresponding measured values of Kc are often higher. A few particles. of copper (Vf -+ 0) in the path of a crack in PMMA, for example, slow down the crack and roughen the fracture surface in the vicinity of the particles and in doing so they raise the fracture toughness as effectively as tungsten wires, despite the extra stiffening effect of the latter[11].

Matrix materials are in most cases isotropic but have different tensile and compressive strengths. Theoretical studies and numerous experiments show that crazing or failure in matrix is sensitive to tensile stress, and different tensile and compressive strengths indicate that matrix failure depends not only on the deviatoric stress invariant, i.e., von Mises equivalent stress VM, but also on the volumetric stress invariant, i.e., the first stress invariant I1. Micro stress invariants in the matrix are calculated as follows:[11]

$$I_1 = \sigma_1 + \sigma_2 + \sigma_3 \tag{5}$$

$$I_2 = \sigma_1 \sigma_2 + \sigma_2 \sigma_3 + \sigma_1 \sigma_3 - (\sigma_4^2 + \sigma_5^2 + \sigma_6^2)$$
 (6)

$$\sigma_{\text{VM}} = \sqrt{I_1^2 - 3I_2} \tag{7}$$

There have been numerous investigations on how such invariants contribute to failure initiation of polymers. If deviatoric and volumetric stresses have a mutually independent effect on failure, the failure criteria could be: [Reference]

$$\frac{\sigma_{\text{VM}}}{\sigma_{\text{VM}}^{\text{cr}}} = 1 \tag{8}$$

However, there are many experimental results revealing the clear interactions between those invariants [38–44]. Since the mechanical behavior of polymers conforms to the definition of isotropy, except for the different tensile/compressive strengths, a simple way to propose failure criteria for polymers is to modify the existing widely used failure criteria for isotropic materials such as the Mohr–Coulumb criterion and generalized von Mises criterion, by incorporating volumetric, or hydrostatic stress into their corresponding expressions. Bowden et al. showed a modified Tresca criterion [42]:

$$\tau_{\text{max}} = S_0 - \mu I_1 \tag{9}$$

where max represents the maximum shear stress in polymer under certain loading conditions; S0 and can be expressed in terms of tensile strength Tm and compressive strength Cm:

$$\mu = \frac{C_{\rm m} - T_{\rm m}}{2(C_{\rm m} + T_{\rm m})} \tag{10}$$

Raghava et al. suggested a modified version of the von Mises criterion [43]:

$$\frac{\sigma_{VM}^2}{C_m T_m} + (\frac{1}{T_m} - \frac{1}{C_m}) I_1 = 1$$
 (11)

2.3.3. Damage of Long Fibres and matrix

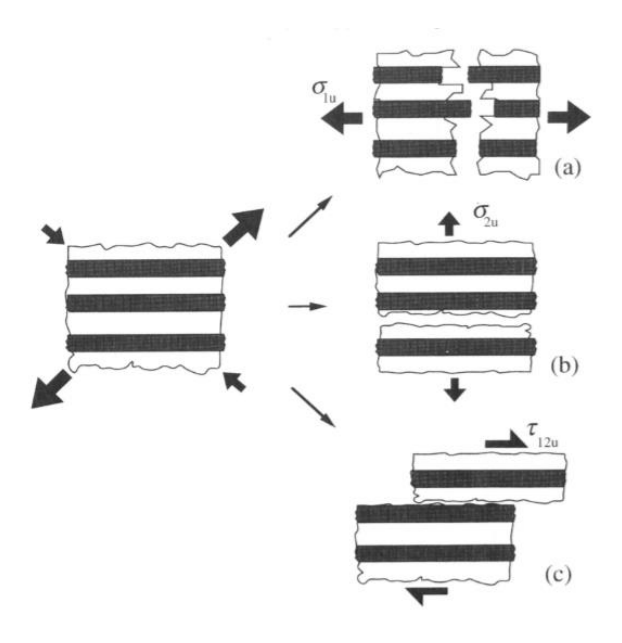


Fig 1.4 Schematic illustration of how an arbitrary stress state in a lamina gives rise to failure as a result of exceeding critical values of (a) axial tensile stress σ_{1u} , (b) transverse tensile stress σ_{2u} and (c) shear stress τ_{12u} [2]

The three most important types of failure are illustrated in Fig. 1.3. Large tensile stresses parallel to the fibres σ_1 , lead to fibre and matrix fracture, with the fracture path normal to the fibre direction. The strength is much lower in the transverse tension and shear modes and the composite fractures on surfaces parallel to the fibre direction when appropriate σ_2 or τ_{12} stresses are applied. In these cases, fracture may occur entirely within the matrix. [2]

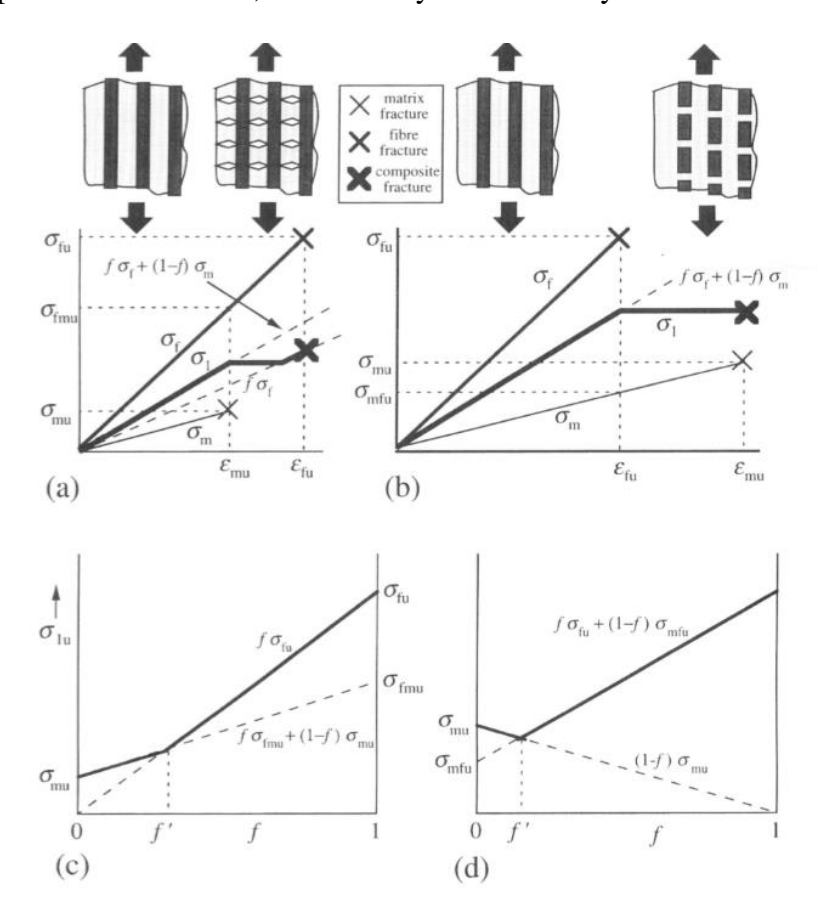


Fig 1.5 Schematic plots for idealised long-fibre composites with both components behaving in a brittle manner. (a) and (c) refer to a system in which the fibre has a higher strain to failure than the matrix and show respectively stress strain relationships (of fibre, matrix and composite) and dependence of composite failure stress on volume fraction of fibre. (b) and (d) show the same plots for the case where the matrix has the higher strain to failure.

In case (a), the matrix has the lower failure strain $(\epsilon_{mu} < \epsilon_{fu})'$ For strains up to ϵ_{mu} , the composite stress is given by the simple rule of mixtures

$$\sigma_m = f\sigma_f + (1 - f)\sigma_m \tag{12}$$

Above this strain, however, the matrix starts to undergo microcracking and this corresponds with the appearance of a 'knee' in the stress strain curve, as shown in Fig. 1.5(a)

Alternatively, if the fibres break before matrix cracking has become sufficiently extensive to transfer all the load to them, then the strength of the composite is given by

$$\sigma_{lu} = f \sigma_{fmu} + (1 - f) \sigma_{mu} \tag{13}$$

where σ_{fm00u} is the fibre stress at the onset of matrix cracking ($\epsilon_1 = \epsilon_{mu}$). The composite failure stress depends therefore on the fibre volume fraction in the manner shown in Fig. 1.5(c). [2] The fibre volume fraction above which the fibres can sustain a fully transferred load is obtained by setting the expression in Eq. (6) equal to $f\sigma_{fu}$, leading to

$$f' = \frac{\sigma_{mu}}{\sigma_{mu} + \sigma_{fmu} + \sigma_{mu}} \tag{14}$$

In case (b), shown in Fig. 1.4(b) and (d), $\varepsilon_{mu} > \varepsilon_{fu}$ the fibres fail first, at a composite strain of ε_{fu} Further straining causes the fibres to break up into progressively shorter lengths and the load to be transferred to the matrix.

Subsequent failure then occurs at an applied stress of $(1-f)\sigma_{mu}$. If matrix fracture takes place while the fibres are still bearing some load, as shown in Fig. 1.5(b), then the composite failure stress is

$$\sigma_{lu} = f \sigma_{fu} + (1 - f) \sigma_{mfu} \tag{15}$$

Where, σ_{mfu} is the matrix stress at the onset of fibre cracking. In principle, this implies that the presence of a small volume fraction of fibres reduces the composite failure stress below that of the unreinforced matrix, as shown in Fig. 1.5(d). This occurs up to a limiting value/' given by setting the right-hand side of Eq. (8) equal to $(1-f)\sigma_{mu}$. [2]

$$f' = \frac{\sigma_{mu} - \sigma_{mfu}}{\sigma_{fu} + \sigma_{mfu} + \sigma_{mu}} \tag{16}$$

2.4. INTERLAMINAR DAMAGE (PROGRESSIVE FAILURE)

In the simplest case, a crack propagating through a well bonded brittle fibre/brittle matrix composite might be supposed to move first through matrix and then through reinforcement,

each with its own characteristic fracture energy, producing a flat fracture surface so that the total fracture energy for the composite was a simple summation of separate component fracture energies. With brittle components this would not be a useful result, for obvious reasons, and fortunately it rarely occurs in practice. Cooper and Kelly 13 showed that in copper reinforced with brittle tungsten wires, catastrophic failure could occur by low energy crack propagation fro~ wire to wire provided the wires were touching so as to provide a continuous crack path. Low-energy failure of this kind can also occur in otherwise tough GRP composites under environmental stress cracking conditions. Unidirectional pultruded GRP rod, for example, is almost impossible to break by propagating a crack normal to the fibres, even under impact conditions with a sharp notch. A notched Charpy specimen simply bends, with disintegration of the resin and multiple interlaminar cracking, until it is forced through the gap between the anvils of the test machine. However, in the presence of acids and under stress as low as one tenth of the failure stress the material will fail by the propagation of a brittle crack from fibre to fibre as successive fibres are rapidly weakened by the acid/stress combination. [8]

Brittle cracking seldom occurs in practical composites under normal conditions, partly because the nature of the interface will usually modify the mode of crack propagation and partly because of the statistical variation of fibre strengths. At any fibre break the load is shed back, via the matrix, to the neighbouring fibres, so that the stresses in these adjacent fibres will be concentrated somewhat above the average fibre stress level (Fig. 1.4). It is statistically improbable, however, that there will be weak spots at the same points in these unbroken fibres, and in the early stages of deformation fibre failures are widely distributed throughout the stressed volume. If the fibre/matrix bond is not too strong some relaxation of the stresses around the broken fibre ends can occur and this, together with local creep relaxations in the matrix, will help to reduce the level of stress concentration in neighbouring fibres. Thus, in GRP, or in CFRP containing high-modulus fibres with low levels of surface treatment, a great deal of fibre damage of this kind may occur before the number of fibre breaks in any crosssection reduces the load-bearing ability of that cross-section below the current level of applied load. The strong fibre/matrix bond prevents relaxation and failure of whole bundles of fibres can occur, the crack spreading from one fibre to the next via the matrix with little or no deviation at the interface, in the brittle mode. [8]

The crack is halted by the fibre, firstly because the high stiffness of the fibre inhibits further opening displacement of the matrix crack at the current level of load, and secondly because the strength of the fibre is too high for it to be broken by the current level of stress concentrated at the tip of the matrix crack. The matrix crack may bow around the fibre, as shown in Fig. 3, but it cannot move past the fibre until the critical matrix COD is exceeded. For further cracking to occur, therefore, some mechanism is required to permit an increased matrix COD. The following discussion is based upon the treatment of Harris et al.18. [8]

As the load applied to the composite is increased, matrix and fibre attempt to deform differentially and a relatively large local stress begins to build up in the fibre. This causes local Poisson contraction which will eventually become sufficiently pronounced to overcome any residual mechanical 'bond' resulting from differential thermal contraction or resin cure contraction. This resistance to shearing at the fibre/matrix interface is derived from a combination of the interfacial shear strength due to chemical bonding and the frictional resistance due to mechanical keying. The effective frictional shear strength of the interface depends on the level of residual compression exerted on the fibres by the resin, and in practical composites this is usually lower than the level of shear strength due to chemical bonding. However, it is very difficult in practice to make sensible measurements of the interfacial shear strengths in real composites. At some critical load, then, the level of shear force developed at the interface (Fig. 1.4 b) will exceed the total static interfacial shear strength and local fibre/matrix debonding will occur at the crack tip. This debonding can travel along the fibre in both directions from the crack tipI8 allowing relative movement of the fibres and matrix (Fig. 1.4c). Further matrix crack opening displacement will therefore occur, resulting in propagation of the matrix crack beyond the fibre.[8]

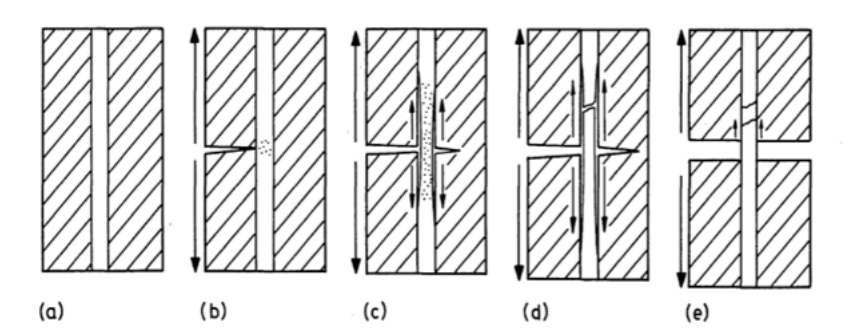


Fig 1.4 (a) Fibre is gripped by resin in uncracked composite (b) Resin crack is halted by fibre (c) Interfacial shearing and lateral contraction of fibre result in debonding and further increment of crack extension (fibre stores elastic strain energy in debonded region) (d) After

considerable debonding fibre breaks at weak spot within resin and further crack extension occurs e Broken fibre end must be pulled out against frictional grip of resin if total separation of sample is to occur. [8]

Frequently a major contributor to the total energy of fracture, especially in the case of GRP, although it is possible that some confusion exists as to the exact nature of the energy absorption mechanism. Debonding requires separation of the fibres from the matrix and this is a process that may be made more difficult by improving the interfacial chemical bond, and vice versa. Outwater and Murphy20 have considered the process as a Mode II cracking phenomenon (similar to that shown in Fig. 1.4e) producing new surfaces at the interface and they have measured values of about 4 kJ m- 2 for the appropriate strain energy release rate for glass/polyester models. If interfacial debonding occurs in preference to cracking within the resin, however, it clearly cannot be a very high energy process and it cannot be assumed to contribute very much more to the composite fracture energy than do the processes of formation of new surfaces in the resin or the fibres. The effect of debonding, however, is to permit a substantial increase in the volume of fibre that is highly stressed and it is more likely to be this mechanism, a consequence of debonding rather than the debonding itself, that adds substantially to the composite fracture energy. Indeed, Harris and Ankara21 have shown that in model glass/polyester composites the overall fracture energy is little affected by the ease or difficulty of debonding. Debonding can, in some circumstances, lead to large-scale deviation of the crack tip parallel to the fibres resulting in an effective blunting of the crack. Cracking may then proceed on some other plane remote from the original crack plane, with a resultant increase in the complexity of the fracture face and an increase in composite toughness acts over a distance equal to the fibre failure extension, suggests that this contribution

$$W_{friction} \approx \frac{N\pi\tau d^2 \varepsilon_f}{2} \tag{17}$$

where ε_f is the fibre failure strain, contributes substantially to the toughness of glass/resin composites. [8]

The surface fracture work of a brittle fibre such as glass makes little contribution to the composite (10J/m2 only). However, the energy required to deform a fibre elastically to its failure load σ_f over its debonded length is substantial. This debonding energy, is $\sigma_f^2/2E_f$ per fibre per unit volume, and this amounts to [8]

$$W_{fibre} = \frac{N\pi\tau d^2\sigma_f^2 y}{8E_f} \tag{18}$$

An interface failure such as debonding or detachment between fiber and matrix can be caused by normal and tangential tractions on the interface. In this study, a quadratic failure criterion in canonical form is used to take into account the interaction between the normal and tangential tractions [15]

$$\left(\frac{t_{\rm n}}{Y_{\rm n}}\right)^2 + \left(\frac{t_{\rm t}}{Y_{\rm t}}\right)^2 + \left(\frac{t_{\rm x}}{Y_{\rm v}}\right)^2 = 1 \tag{19}$$

where angular brackets h i stand for the Macaulay brackets, which return the argument if positive and zero otherwise, so that there will be no damage at the interface when the interface is under compression. tn, tt, and tx indicate interfacial tractions in normal, tangential (to the circumference), and longitudinal directions, respectively, while Yn, Yt, and Yx represent the maximum allowable values of interfacial traction in those three directions, respectively. Considering the overall effect of interfacial shear traction, Equation (16) can be rewritten in the form: [15]

$$(\frac{t_n}{Y_n})^2 + (\frac{t_s}{Y_s})^2 = 1 \tag{20}$$

in which ts and Ys represent interfacial shear traction and interfacial shear strength, respectively. When the interface failure condition is met, complete detachment between the fiber and the matrix may not occur instantaneously. Rather, the interface will undergo a process of property degradation, until the ultimate detachment occurs. A simple schematic illustration of the typical traction-separation law describing the interface behavior can be found in references [46,47]. In each direction (normal, tangential, or longitudinal), before the maximum allowable traction is reached, the separation between fiber and matrix is directly proportional to traction; after traction reaches its maximum allowable value, if separation continues to increase, the corresponding traction value will linearly decrease until zero, after which complete detachment can be achieved. [15]

3. Practical part

Many researchers have used different technique for the measurement of stress, deformation and strain on composites at different load condition. In this study, the effect of stress and strain are studied on cylindrical fibres reinforced in a box shaped matrix and analysed what happened when fiber fail first and matrix fail first. The properties of composites depend not only on the properties of the fibers and matrix, but also on the reinforcement method. This analysis is done on unidirectional fibre composites. The greatest parameters of mechanical properties are unidirectional composites when loaded along fibers. Strength and modulus of elasticity along the fibers increase with increasing the content of fibers in the composition, and up to a certain limit, due to the density of packing fibers in the composition, ensuring preservation of the monolithic binder.

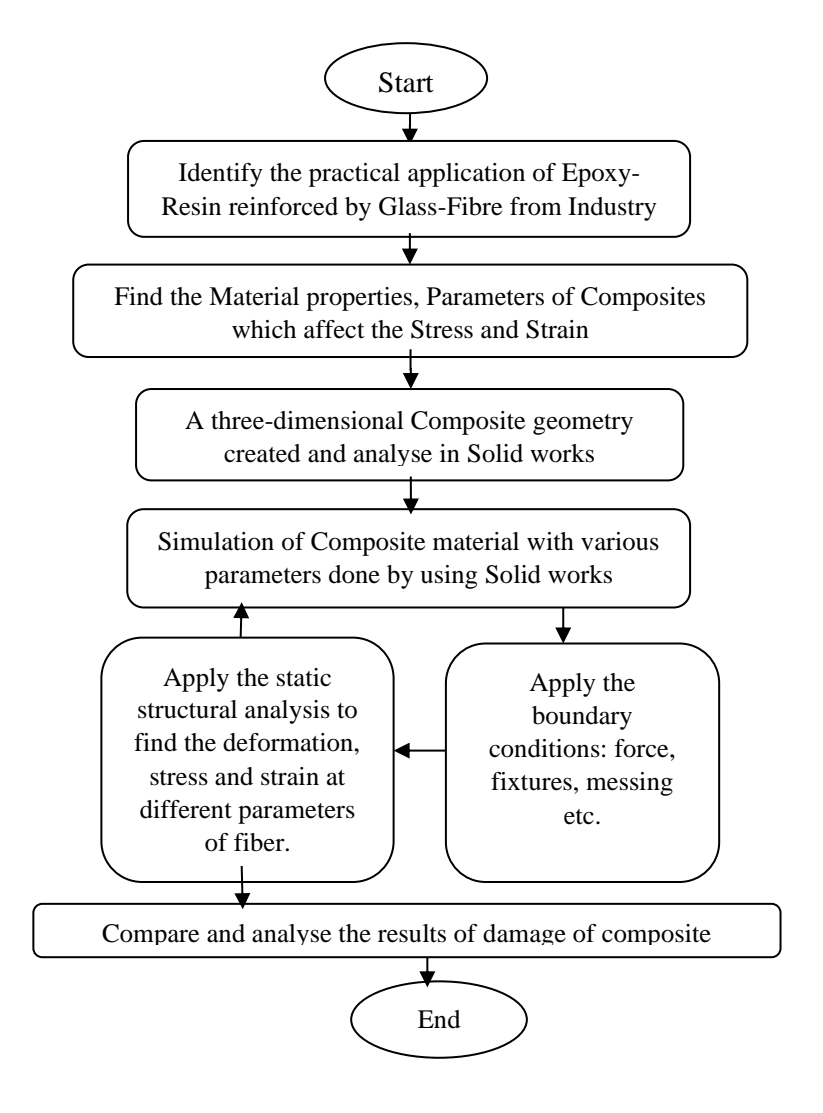


Fig 3.1 Flow chart showing the steps performed in this analysis

A three-dimensional computer aided design modelling in longitude direction under tensile loading is done with the help of SOLIDWORKS 2019. Glass-Fibre and Epoxy-Resin are used as materials for the fibre and Matrix respectively. The definition of physical properties (elastic modulus, Poisson's ratio) of composite material is a necessary factor for setting up the model.

Mechanical properties for the matrix and fiber are described in table 3.1.

Table 3.1

Main geometry data for testing

Fibre material	Glass fibre
Matrix material	Epoxy-Resin
Elastic modulus of epoxy resin	4 GPa
Elastic modulus of glass fiber	72 GPa
Poisson's ratio of epoxy resin	0.35
Poisson's ratio of glass fiber	0.22

3.1. Fiber Failure (Damage applying in fiber)

Fiber failure simulation is performed using Solid works software. The geometrical dimension, boundary conditions, material properties is defined accordingly. Firstly, static simulation of fiber failure is carried out in order to understand the stress distribution in the composites. The results are obtained, and suitable comments are providing accordingly.

Assumptions:

Here, all parameters were obtained in one direction because displacement applied only on single direction and, so further all analysis and simulation obtained on single direction.

The following assumptions were made in all simulation treatment

- 1. All simulation defined under Macroscopic analysis.
- 2. Only one element is calculated during one step of simulations.
- 3. For next results is carried out by choosing the fiber where next maximal average stress obtained.
- 4. During the simulations, control the stress of composites.

3.1.1 Structure of composites

At the beginning of structure, on the front plane, a rectangle with height 50 mm and length 50 mm is created. After that, using Extruded Boss/Base features with width 20 mm, 2D rectangle substituted in 3D cube and apply modified Epoxy resin as a material. The structure of model in figure 3.1.

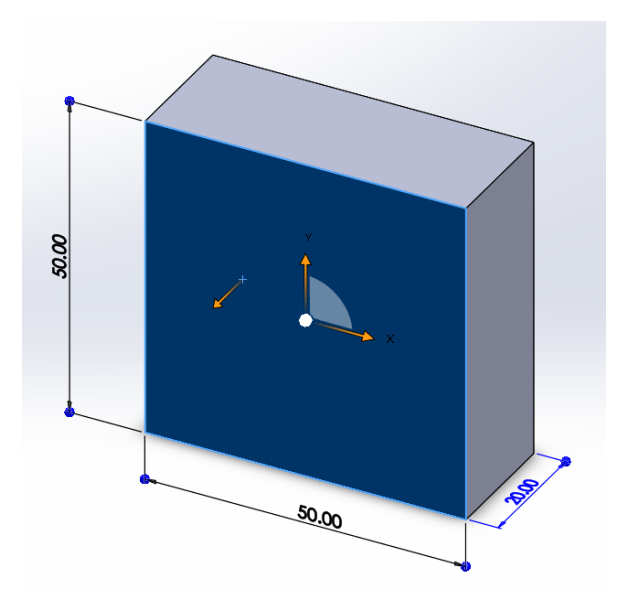


Figure 3.1. Cubic matrix

Then after, on top plane, 13 circles with diameter 0.75 mm are created and distance between each 13 circles is 3.5 mm. After, using Extrude Cut feature with depth 50 mm, created 13 cylindrical shaped holes for reinforced Fiber. The structure of matrix with hole in figure 3.2.

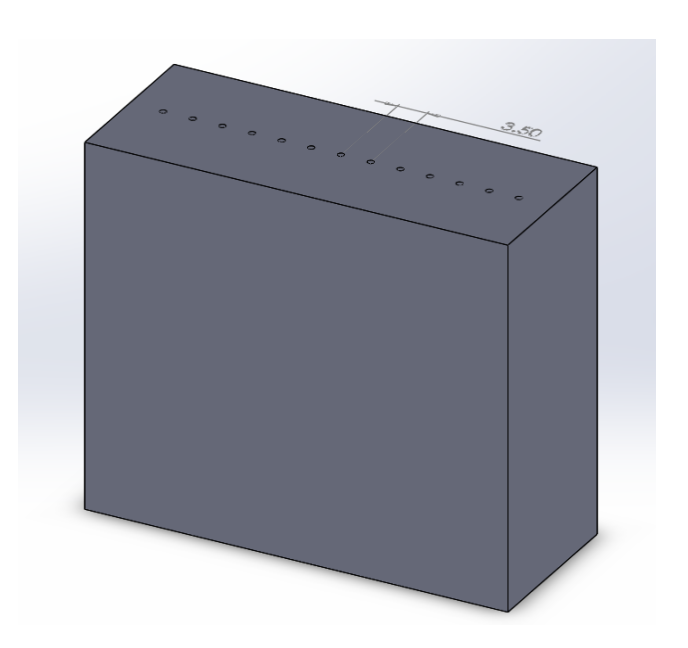


Figure 3.2. Holes in Matrix model

Then created 13 cylindrical fibers as a reinforce material with diameter 0.75 mm and height 50 mm and applied modified Glass fiber as a material. In figure 3.3, glass fiber



Figure 3.3. Cylindrical-shaped glass fiber

After assembled the structure of basic Model of Matrix and Glass fibre is shown in figure 3.4.

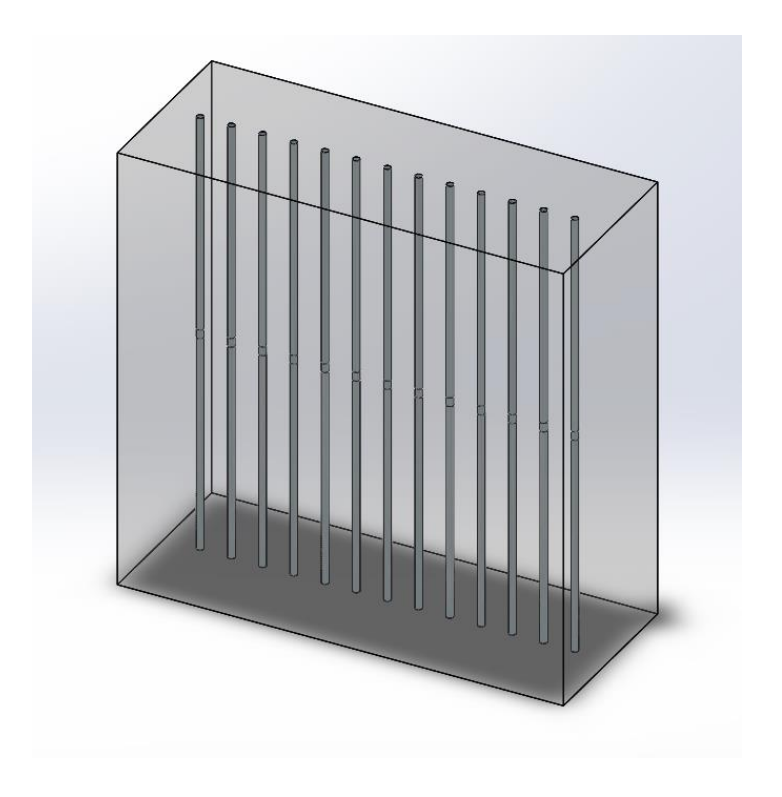


Figure 3.4. Final model of composites (with matrix transparency)

3.1.2 Applying Boundary Condition

Roller Slider was used for restriction to establish that a flat face can move freely in its plane but cannot move in a direction perpendicular to its plane. The face can shrink or expand under load/displacement and is shown in figure 3.5.

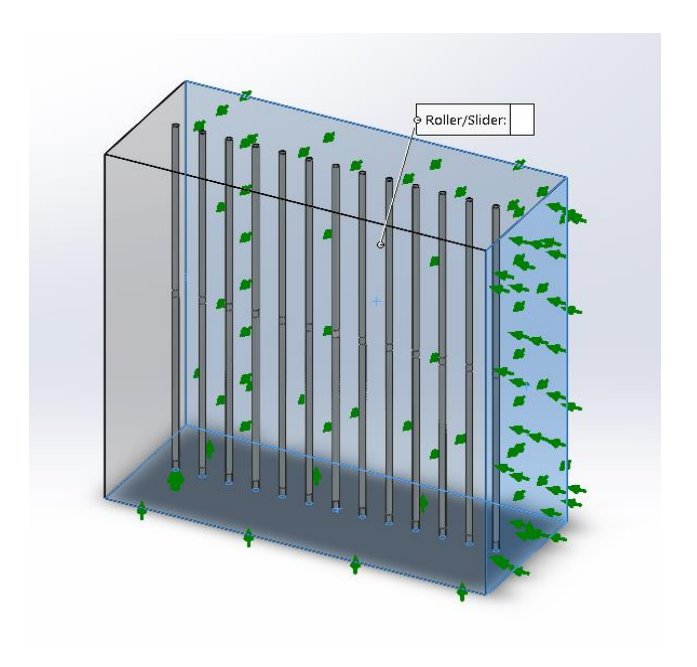


Figure 3.5. Slides where roller slider applied

In this simulation a displacement in amount of 1 mm on the top side of a model was given Instead of applying force as shown in figure 3.6.

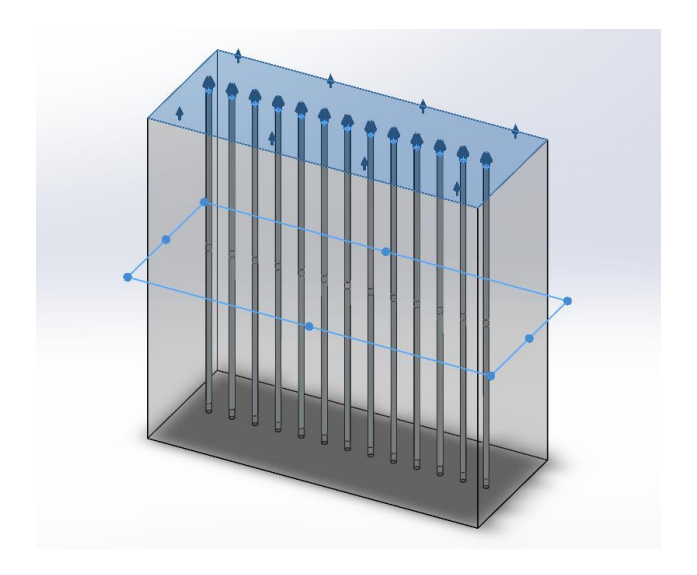


Figure 3.6. plane where displacement 1 mm applied

Meshing is done to discretize the geometry into elements and nodes spatially. In this assembly curvature-based mesh as a mesher used and Solid mesh type mesh is used for discretization of model and is shown figure 3.7.

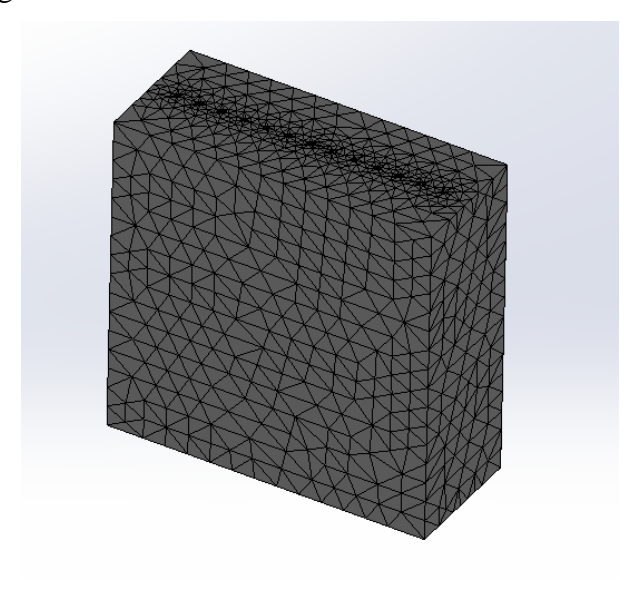


Figure 3.7. composites with mesh

3.1.3 Results after simulation

After simulation was done by Solid works, result and graph for stress, displacement and strain were defined and all are shown in blow figure 3.8 to 3.10 respectively.

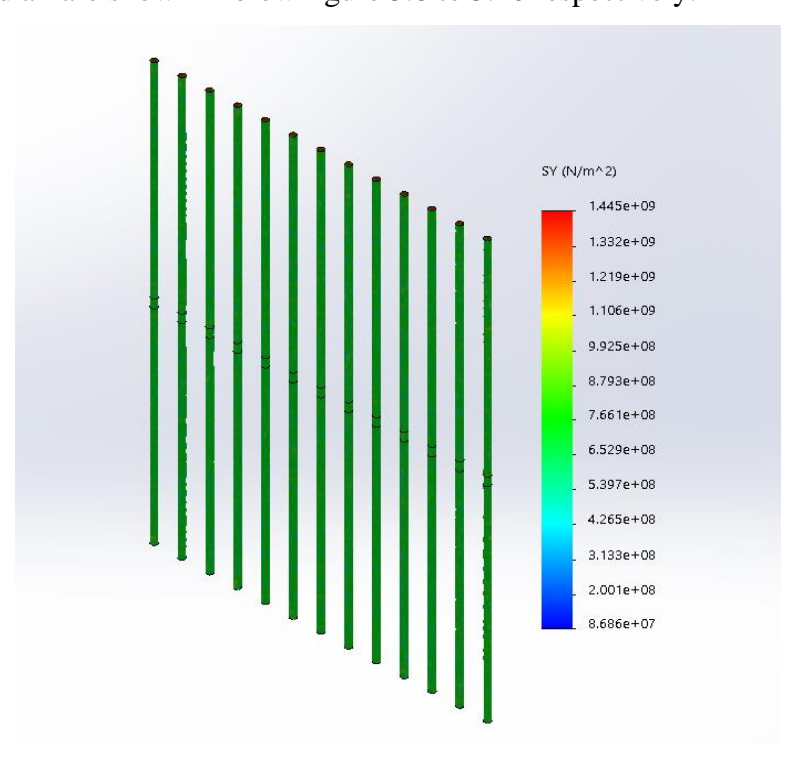


Figure 3.8. stress plot in Y direction in composites

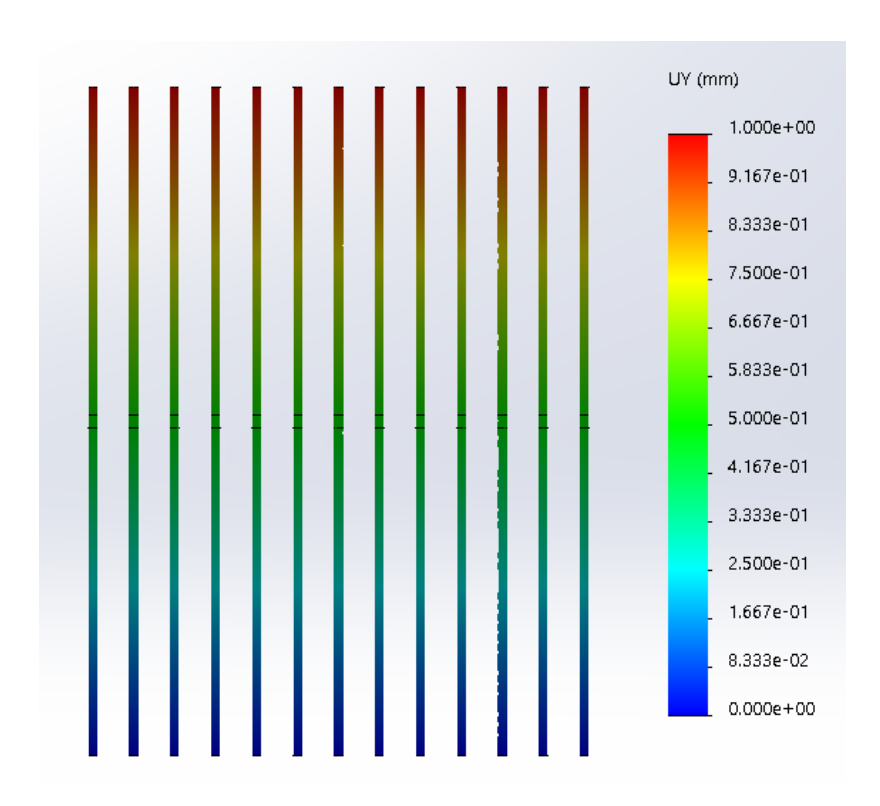


Figure 3.9. displacement plot in Y direction in composites

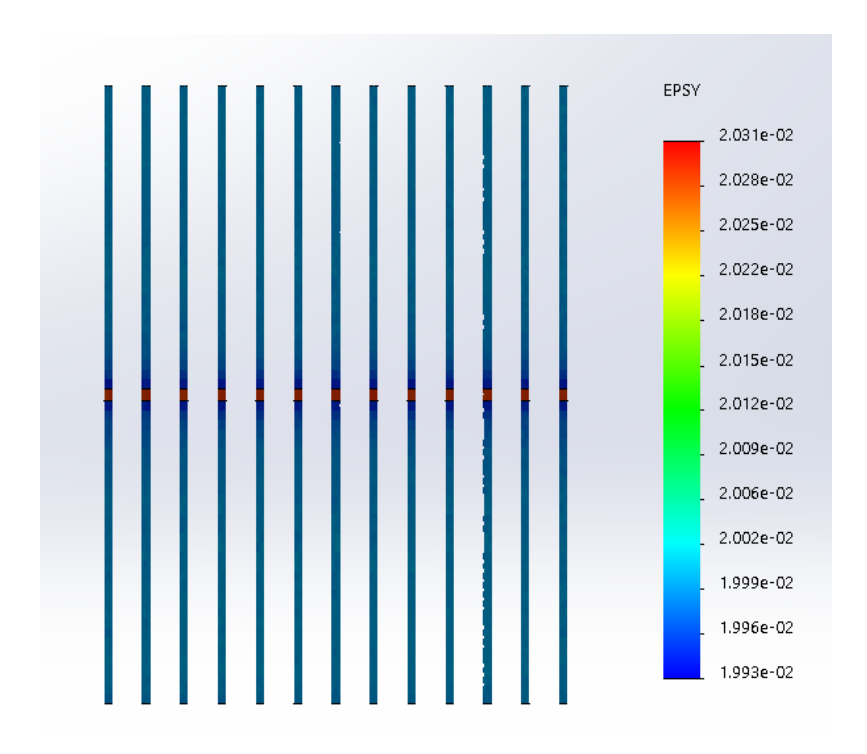


Figure 3.10. strain plot in Y direction in composites

According to assumption and from simulations results, stress analysis is defined at the centre (it shown in figure 3.3) of all 13 fiber without considering any damage to find average stress

at each fiber. The all 13 elements on which stress analysis is performed is 1 mm in height (centre part, see figure 3.3). Analysing the stress result by performing static simulation, it is possible to predict where damage or break can take place in composites. When there is no damage, the average stress acting on all the middle part of the fiber in composites can be calculated by adding the individual stress on each element divide by total number of all elements. The graph below (figure 3.11) shows the stress at the middle element of the each fiber.

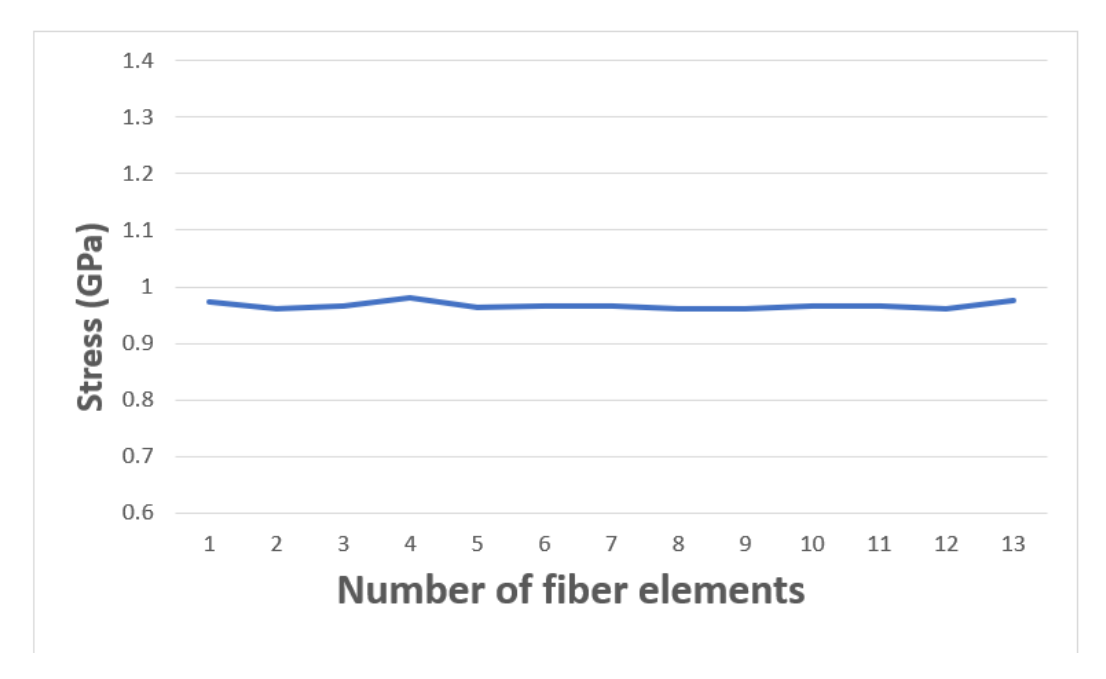


Figure 3.11. Stress graph for centre of fiber elements (numbers from left to right)

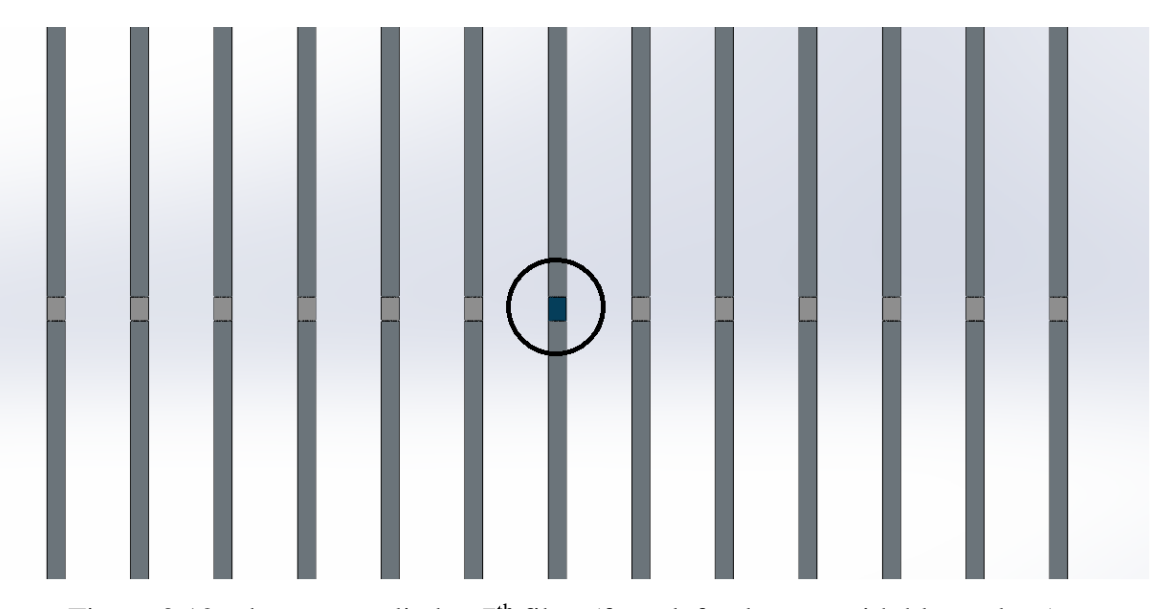


Figure 3.12. damage applied at 7th fiber (from left, element with blue colour)

Now, stress analysis is performed by considering damage in centre part of the fiber. First, the 7th fiber element (from left) is considered and damage is applied at centre of fiber. But in model, it is not possible to show the damage, so we will insert a new material which has modulus of elasticity is equal to 1 MPa (see figure 3.12) for applying damage. According to our assumption, after applying damage on 7th element, it is expected that the maximum stress will be on one of the next elements located on either side of 7th element (either 6th or 8th). The stress acting on either 6th or 8th element after fracture should be greater than the average stress obtained without considering any damage. Again, the damage is applied on the fiber element (either 6th or 8th) which has maximum stress, along with the damage which is already applied on 7th element.

Static simulation is performed for the damage in 7th element, stress plot is obtained (figure 3.13). According to the result obtained in graph, it can be said that maximum stress obtained on 6^{th} fiber element. So, now the damage is applied on 6^{th} fiber element along with the damage on 7^{th} fiber element. As per our assumption, the maximum stress should be on either 5^{th} or 8^{th} and the average stress acting on these elements should be greater than the stress acting on 6^{th} element.

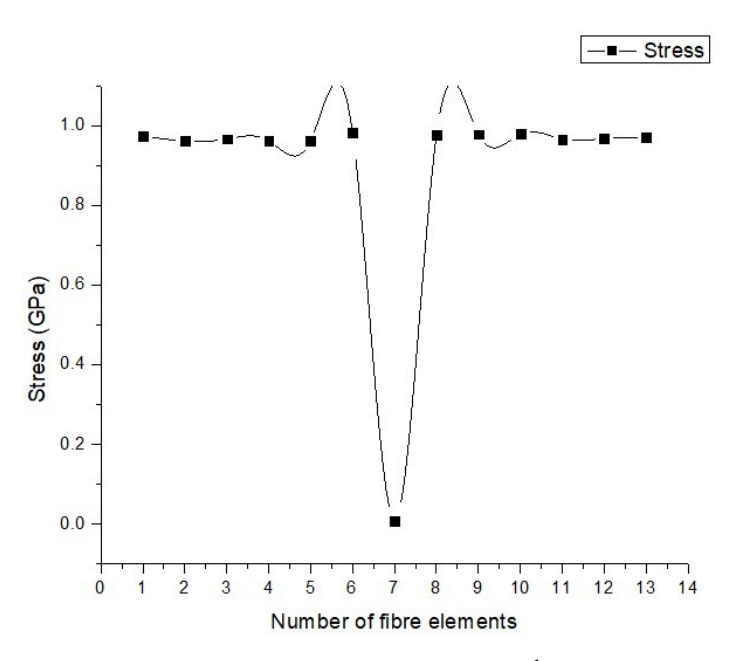


figure 3.13. stress plot after fracture of 7th fiber element

Again, same procedure is repeated, static analysis is performed when fiber elements number 6th and 7th are fractured, stress plot is obtained (figure 3.14). According to the result obtained in graph, it can be said that maximum stress obtained on 5th fiber element. So now, the

damage is applied either on 4th or 8th fiber elements. The same procedure is repeated continuously for the other remaining fiber element. Each fiber element is damaged one by one until all 13 fiber elements are damaged. For performing static analysis considering the fracture in every new element, the previous fracture element is also taken into consideration.

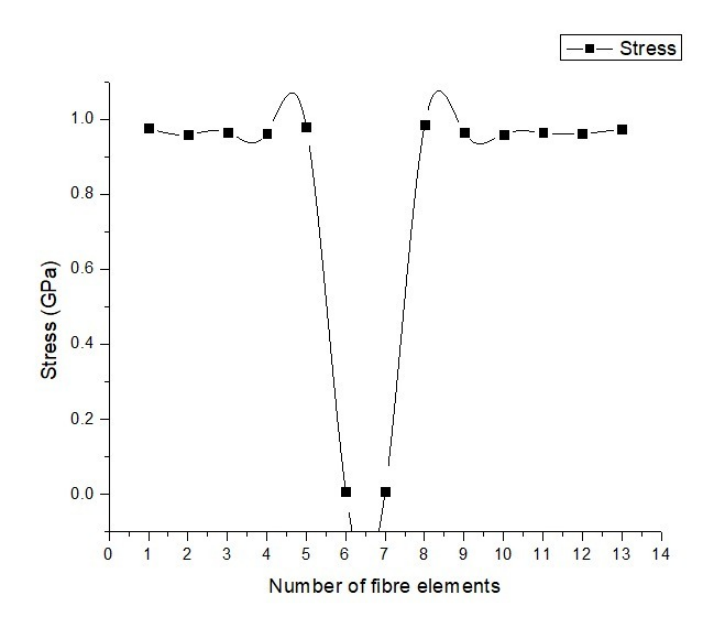


Figure 3.14. stress plot after fracture of 6th & 7th fiber element

The sequence in which the fracture is applied on fiber element is as follows and the stress acting after applying fracture on fiber elements is described in table 3.2.

Table 3.2

Number of damages fiber	Sequence in which the fiber	Stress (GPa)
element	elements are damaged	
0	-	0.9668
1	7	0.9841
2	6	0.9814
3	5	0.9846
4	8	0.9795
5	4	0.9844
6	3	0.9848
7	2	0.9916
8	1	0.9760

9	9	0.9813
10	10	0.9849
11	11	0.9763
12	12	0.9926
13	13	-

Using the information, which is given in table 3.2, the graph between number of damages fiber elements and Stress (GPa) is plotted. According to our assumption, the plot should be in increasing order. i.e. when number of damages fiber element increases, the stress acting on the corresponding fiber elements should also be increased. But from the graph, which is given in figure 3.15, shows that it is increasing as well as decreasing. This fails our assumptions.

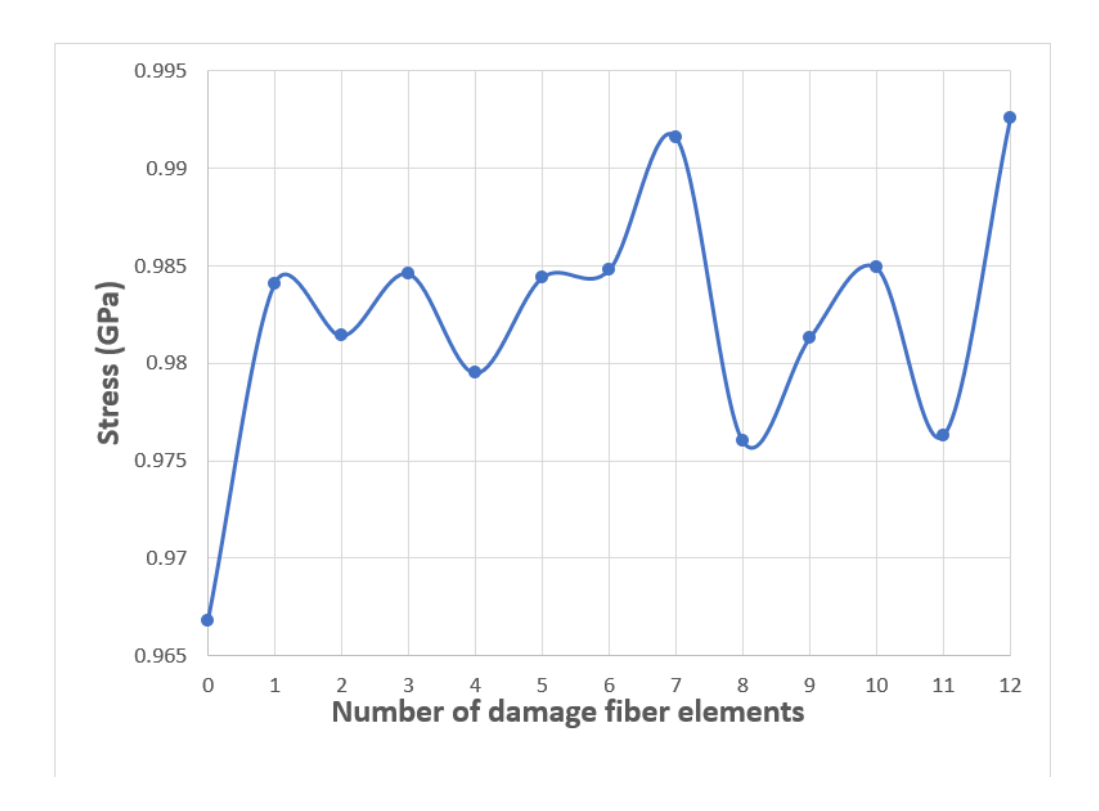


Figure 3.15. plot between number of damages fiber elements and stress

One of the reasons for such graph is, according to the theory of damage of composites, first always matrix failure take place and then fiber damage start. So, static simulation for the model 1 in which first fiber fails in composites is not accurate. In the further part of the work

the damage of matrix take place first, static simulation is performed by creating a new virtual model in Solid works and results are analysed.

3.2 Matrix Failure (Damage applying in matrix)

Now, we will consider the matrix failure simulation for two different model which is created using solid works software. The geometrical dimension for matrix for both the model is same, whereas the geometrical dimension for fiber is different for both models. The fiber dimension for model 1 is, diameter = 0.25 mm and height = 0.50 mm, for model 2, diameter = 0.125 mm and height = 0.50 mm.

Assumptions:

Here, all parameters were obtained in one direction because displacement applied only on single direction and, so further all analysis and simulation obtained on single direction for both models.

The following assumptions were made in further simulation treatment.

- 1. All simulation defined under Macroscopic analysis.
- 2. Matrix and fibers failure happen only in the one considered plane.
- 3. Matrix and fiber failure simulation is carried out by switching off symmetry boundary conditions for elements with next maximal average stress.
- 4. Only one element is switching out during one step of calculation.
- 5. Controls of failure stress and failure strain for each fiber for each step.

The details explanations about geometrical characteristics, boundary conditions and static simulation results are given below:

3.2.1 Structure of model 1

Here first, on the front plane, a rectangle with height 0.50 mm and length 1.50 mm is created at the beginning of the Model. After that, using Extruded Boss/Base features with width 0.50 mm, 2D rectangle substituted in 3D cube and apply modified Epoxy resin as material. The structure of model in figure 3.16.

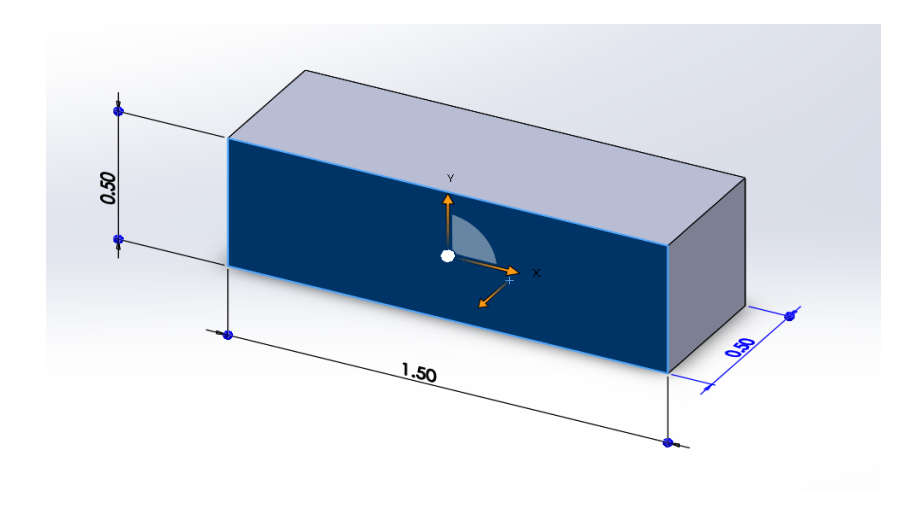


Fig. 3.16. structure of cube model 1

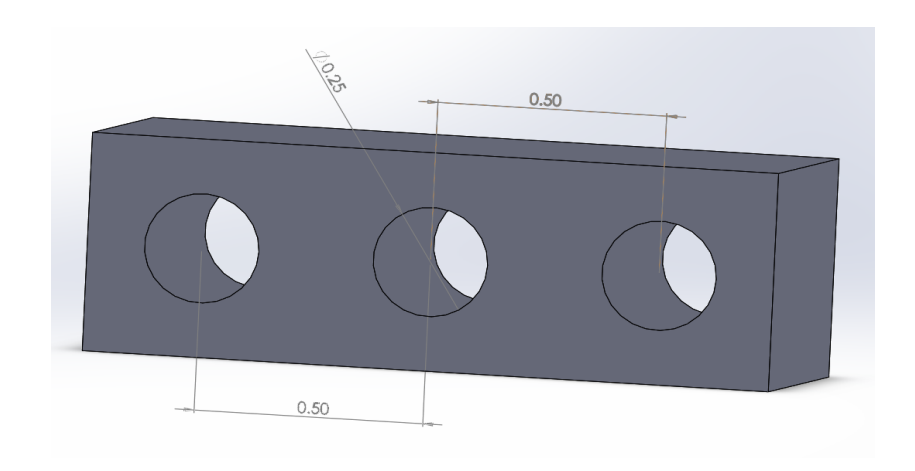


Fig. 3.17. 3 holes in epoxy matrix

Then after, on front plane, 3 circles with diameter 0.25 mm are created and distance between each 3 fiber is 0.50 mm. After, using Extrude Cut feature with width 0.50 mm and created 3 cylindrical shaped holes for reinforced Fiber. The structure of matrix with hole in figure 3.17.

Split the parts in Solid works

Before making final assembly, here used Split features for accurate simulation, because split tool is a useful and enormously feature when designing using multi body part techniques in Solid works [51]. Split feature easily breaks the target surfaces or plane in multiples bodies. This preserves the original shapes of materials and just divided into manifold parts.[52]

Here, using split feature, divided Matrix model with holes in $0.625 \text{ mm} \times 0.625 \text{ mm}$ square parts and that all parts are working as their own properties when command applied on that. Using split and trim feature, created sketch in figure 3.18.

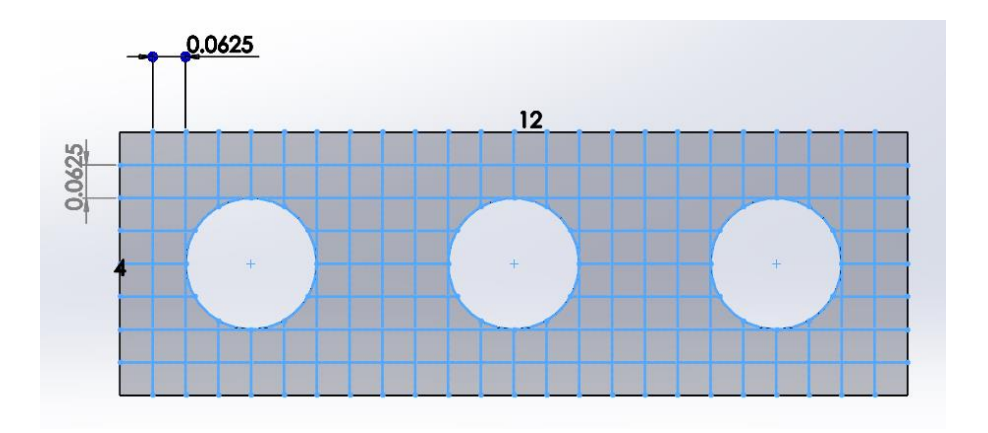


Figure 3.18. sketch for split tool in Solid works

After applied split tools in model, front, side, top and isometric view in figure 3.19.

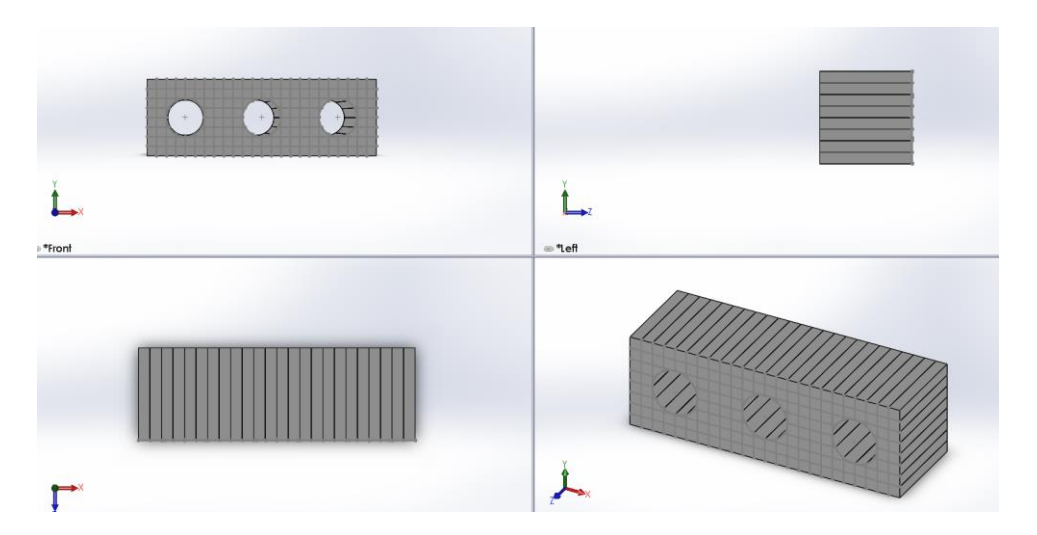


Figure 3.19. Front, side, top and isotropic view after applied split feature

Then created 3 cylindrical fibers as a reinforce material with diameter 0.125 mm and height 0.50 mm and applied modified Glass fiber as a material. In figure 3.20, glass fiber

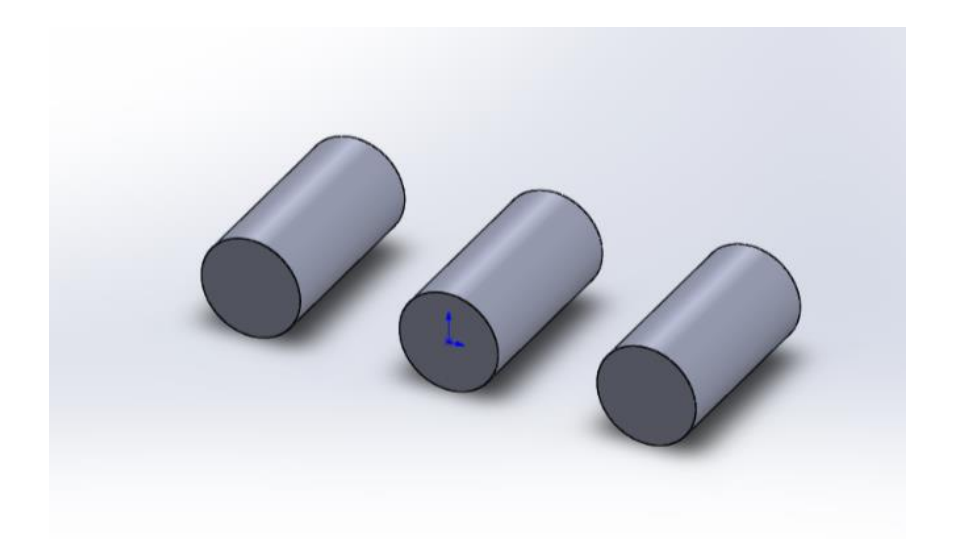


Figure 3.20. Cylindrical shaped Glass fiber as a reinforced

The structure of model 1 is shown in fig 3.21.

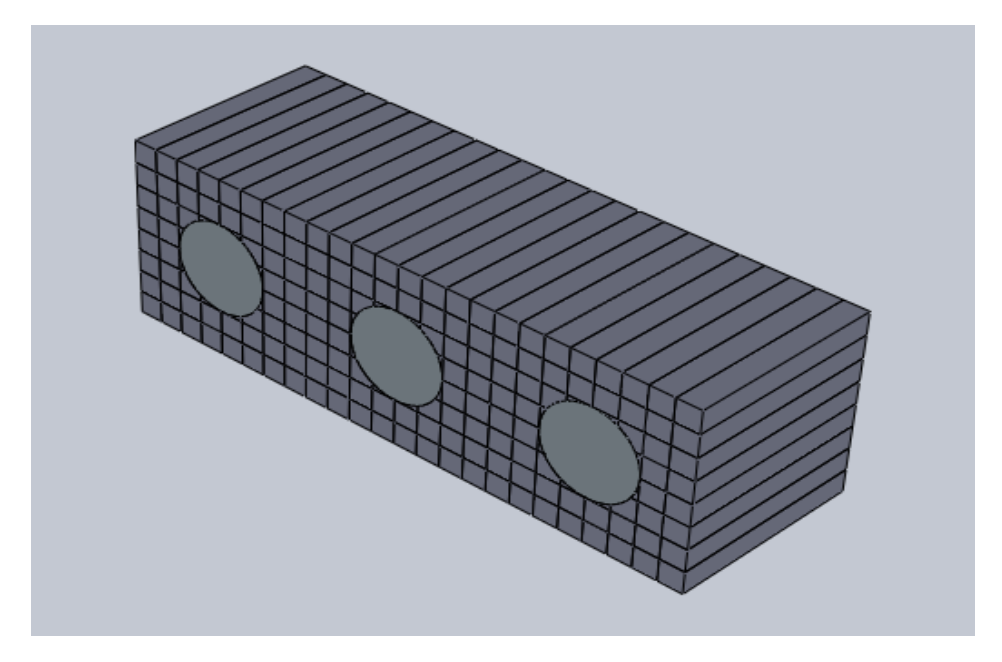


Fig 3.21. Complete Modal of Matrix and Glass fibre

Applying Boundary Condition

Meshing is done to discretize the geometry into elements and nodes spatially. In this assembly Solid mesh type mesh is used for discretization of model and the size is 0.0310732 mm with the ratio of 1.4. It is shown in figure 3.22.

Total element = 14074

Total no. of nodes = 20886

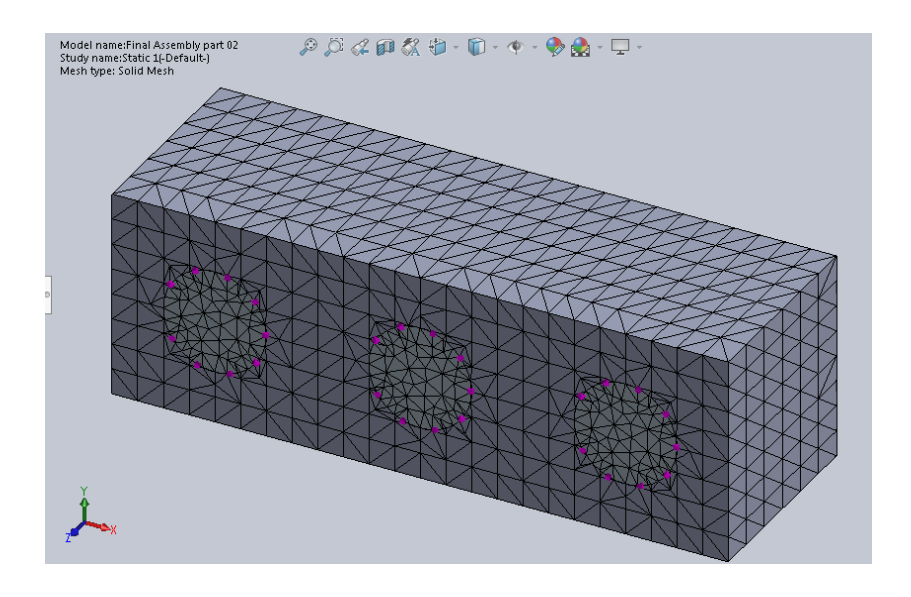


Fig. 3.22. Meshed model of Matrix and Glass fiber.

Roller Slider was used for restriction to establish that a flat face can move freely in its plane but cannot move in a direction perpendicular to its plane. The face can shrink or expand under load and is shown in figure 3.23.

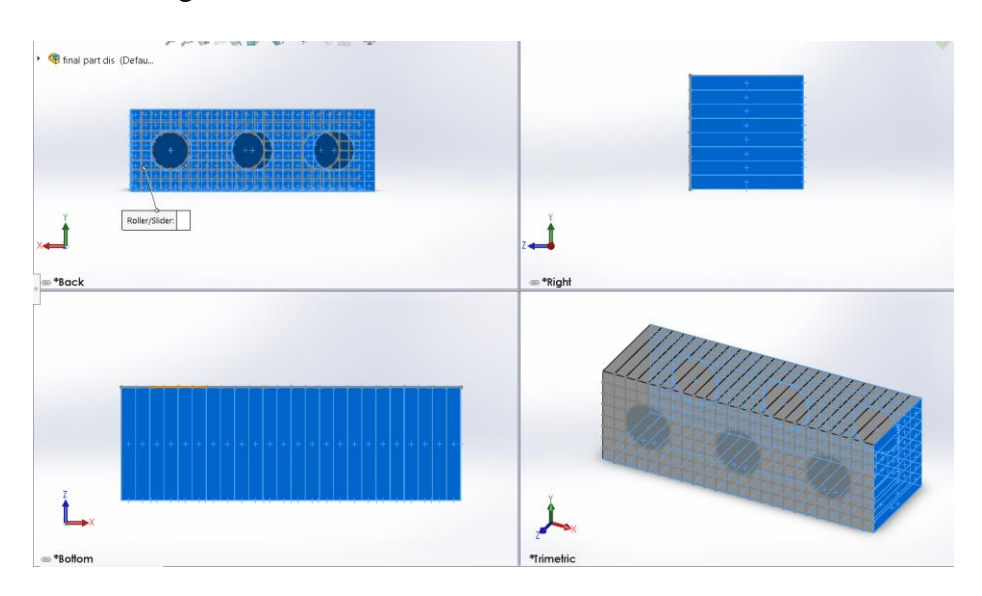


Fig 3.23. roller slider is applied on bottom, right and back plane

For the static simulation, displacement of magnitude 0.012 mm is applied in the positive Z direction instead of applying load (figure 3.24)

The post processing operation is carried out in the SOLIDWORKS software after developing the model, discretizing and solving the governing equations by incorporating the appropriate boundary conditions.

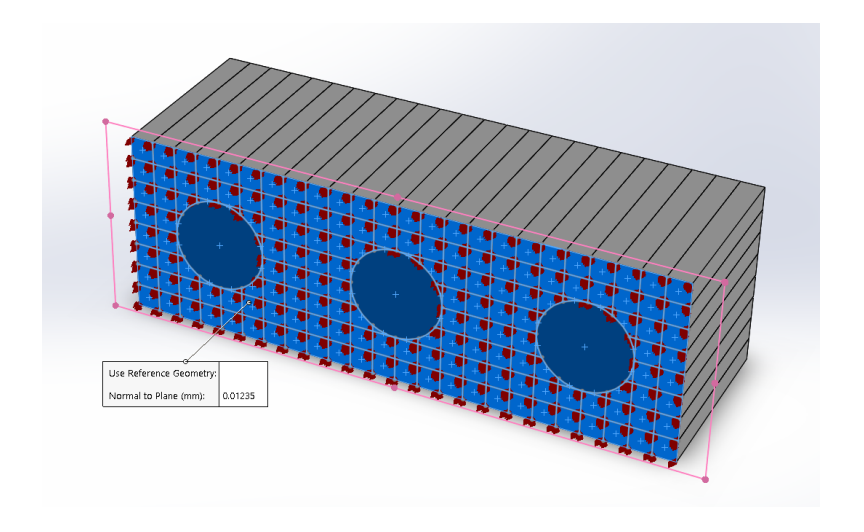


Figure 3.24. face where displacement of 0.012 mm was applied

Results of Simulation

After simulation was done by Solid works, result and graph for stress, displacement and strain were defined and all are shown in below figure 3.25 to 3.27 respectively.

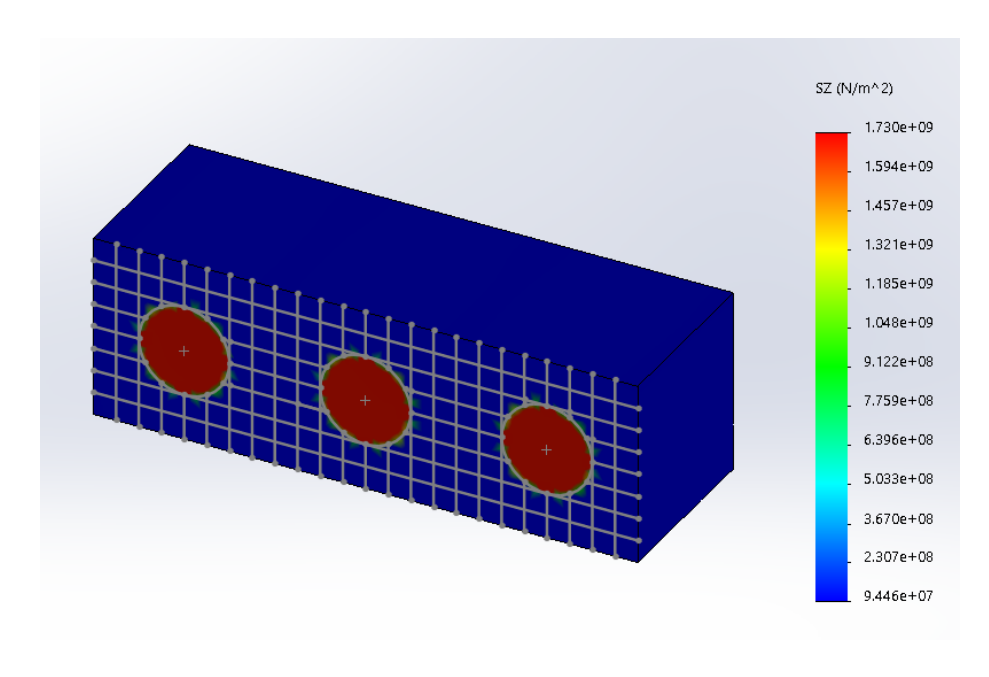


Figure 3.25. Stress plot in Z directions

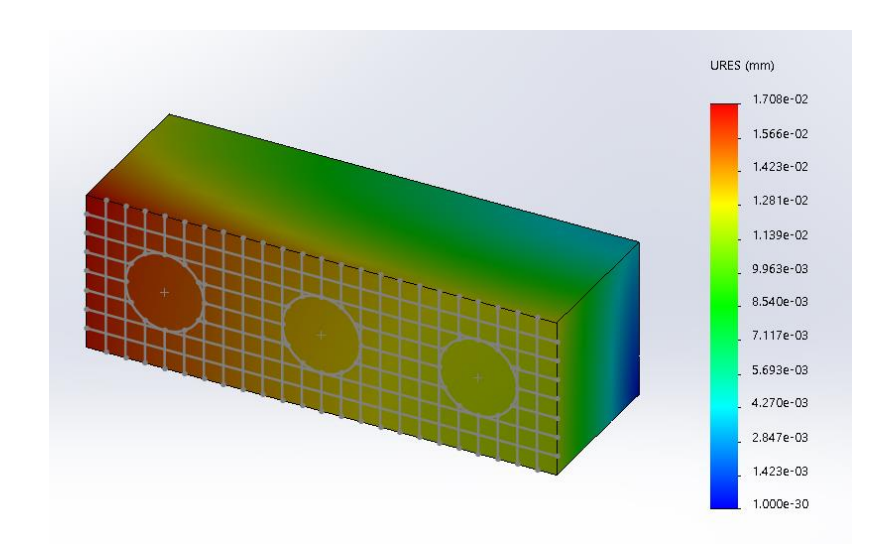


Figure 3.26. Displacement plot in Z direction

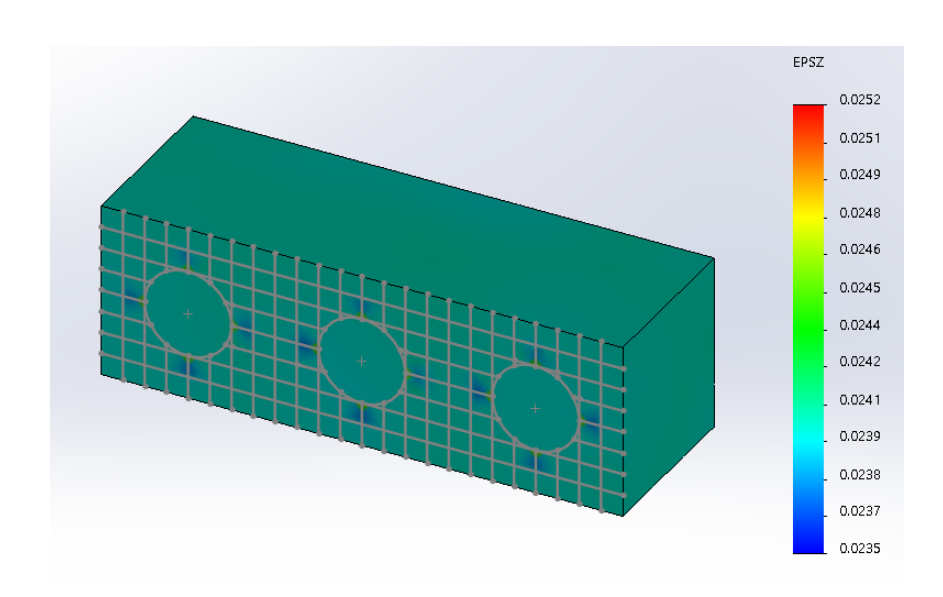


Fig 3.27. Strain plot in Z direction

Applying failure under tensile loading in model 1

The matrix is divided into several smaller elements using spilt feature (figure 3.19). According to assumption, step 1, the stress is applied on the single element which is located between fiber 1 and 2 from left side and on the back side of the model where roller slider is applied as shown in figure 13. Generally, the damage is applied on any elements which are given, but one of the reasons for applying damage on that particular elements which is shown in figure 3.28 is that, the element has maximum stress of around 0.098 GPa (close to failure

stress of epoxy resin, 0.1 GPa) and also that element is located between the two fibers, not too close to them.

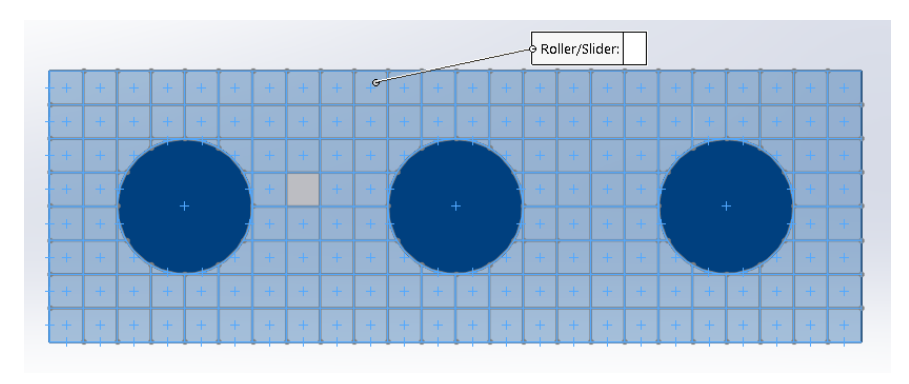


Fig 3.28 one element selected for damage

Matrix failure simulation is carried out by switching off symmetry boundary conditions for selected element with maximal average stress. Static simulation is performed using solid works software and results are noted. The stress acting on all the three fibers is also taken into consideration while taking the results. The next element on which failure is applied is decided by looking at the maximal average stress acting on element. So, the element on which the maximum average stress is acting, on that element next failure is applied and taking into consideration the previous failure along with it. Step 2, by looking at the results, the next elements on which failure is applied is left of the previous element and right side of fiber 1 (from left side) as shown in figure 3.29. The average stress acting on that element is 0.1062 GPa. Again, the matrix failure simulation is carried out by switching off symmetry boundary conditions for the selected two elements with maximal average stress. Static simulation is performed, and results are noted. Again, all the steps are repeated, the element with maximal average stress is selected and failure acts on it, the boundary conditions are switched off for that element and matrix failure simulation is performed. This all steps are repeated until composites fails. It is noted from the results, that composites fail after performing 83 steps by selecting 83 individual split elements one by one.

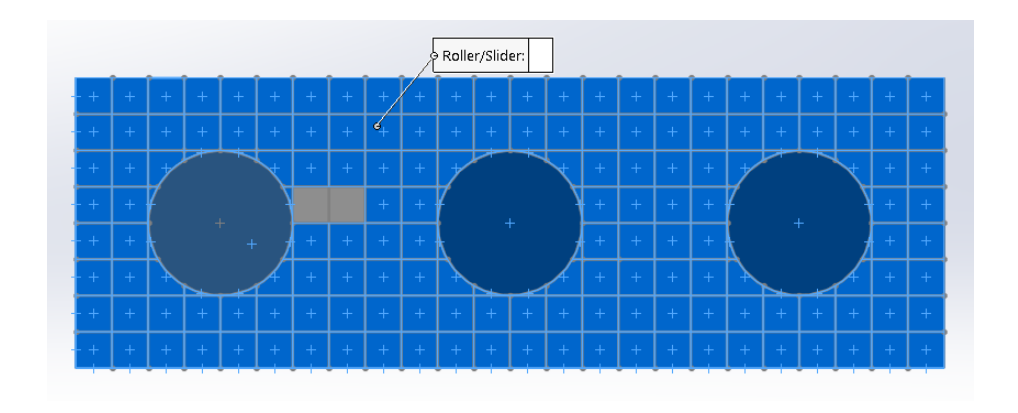


Fig 3.29. two elements selected for damage

The matrix failure simulation for all 83 steps, the stress of matrix and the stress of left, center and right fiber, are given below table 3.3.

Table 3.3

	Location of elements		Felements Stress (GPa)				
Steps	Row	Column	Matrix	Left Fiber	Centre fiber	Right fiber	
1	4	8	0.097	1.703	1.703	1.703	
2	4	7	0.1062	1.705	1.703	1.703	
3	4	6	0.1062	1.706	1.703	1.703	
4	5	8	0.1222	1.707	1.703	1.703	
5	5	7	0.1120	1.712	1.704	1.703	
6	4	9	0.1200	1.712	1.704	1.703	
7	5	9	0.1216	1.713	1.705	1.703	
8	6	8	0.1257	1.714	1.705	1.703	
9	6	9	0.1287	1.715	1.706	1.703	
10	6	7	0.1393	1.720	1.706	1.703	
11	5	6	0.1269	1.720	1.707	1.703	
12	7	8	0.1295	1.721	1.707	1.703	
13	7	7	0.1376	1.723	1.707	1.703	
14	7	9	0.1347	1.724	1.708	1.703	
15	8	8	0.1463	1.724	1.708	1.703	
16	8	7	0.1652	1.726	1.709	1.703	
17	8	9	0.1540	1.727	1.71	1.703	
18	8	6	0.1707	1.729	1.71	1.703	

	Location	of Elements		Stress (GPa)			
					Centre		
Steps	Row	Column	Matrix	Left fiber	fiber	Right fiber	
19	7	6	0.1723	1.734	1.71	1.703	
20	6	6	0.1550	1.746	1.71	1.703	
21	8	5	0.1622	1.749	1.71	1.703	
22	7	5	0.1833	1.757	1.711	1.703	
23	6	5	0.1566	1.761	1.711	1.703	
24	8	10	0.1813	1.762	1.711	1.703	
25	7	10	0.1799	1.764	1.714	1.703	
26	6	10	0.1683	1.765	1.718	1.703	
27	5	10	0.1724	1.766	1.725	1.703	
28	5	11	0.1610	1.766	1.725	1.703	
29	8	11	0.1823	1.767	1.727	1.703	
30	7	11	0.1931	1.768	1.732	1.703	
31	6	11	0.1532	1.769	1.746	1.703	
32	8	12	0.1673	1.769	1.749	1.703	
33	7	12	0.1951	1.769	1.758	1.703	
34	6	12	0.1522	1.769	1.762	1.703	
35	4	10	0.1523	1.770	1.770	1.703	
36	8	4	0.1506	1.773	1.77	1.703	
37	7	4	0.1463	1.783	1.77	1.703	
38	8	3	0.1497	1.785	1.77	1.703	
39	7	3	0.1658	1.792	1.771	1.703	
40	6	4	0.1468	1.793	1.771	1.703	
41	8	2	0.1503	1.795	1.771	1.703	
42	7	2	0.1533	1.799	1.771	1.703	
43	8	1	0.1818	1.801	1.771	1.703	
44	7	1	0.1715	1.805	1.771	1.703	
45	6	3	0.1699	1.814	1.771	1.703	
46	6	1	0.1969	1.817	1.771	1.703	
47	6	2	0.1651	1.831	1.771	1.703	

	Location of	of elements		Stress (GPa)			
					Centre		
Steps	Row	column	Matrix	Left fiber	fiber	Right fiber	
48	5	1	0.1751	1.834	1.771	1.703	
49	5	2	0.1946	1.844	1.771	1.703	
50	5	3	0.1549	1.849	1.771	1.703	
51	4	1	0.1501	1.852	1.771	1.703	
52	4	2	0.145	1.861	1.771	1.703	
53	3	1	0.1479	1.864	1.771	1.703	
54	3	2	0.1778	1.87	1.771	1.703	
55	4	3	0.1462	1.871	1.771	1.703	
56	2	1	0.1496	1.873	1.771	1.703	
57	2	2	0.1465	1.876	1.771	1.703	
58	1	1	0.1763	1.878	1.77	1.703	
59	1	2	0.1673	1.881	1.77	1.703	
60	2	3	0.1808	1.883	1.77	1.703	
61	1	3	0.2021	1.888	1.77	1.703	
62	3	3	0.1638	1.905	1.77	1.703	
63	1	4	0.1841	1.907	1.77	1.703	
64	2	4	0.2224	1.917	1.77	1.703	
65	3	4	0.1561	1.924	1.769	1.703	
66	1	5	0.1617	1.926	1.769	1.703	
67	2	5	0.145	1.936	1.769	1.703	
68	1	6	0.1552	1.937	1.769	1.703	
69	3	5	0.533	1.938	1.769	1.703	
70	2	6	0.1448	1.944	1.769	1.703	
71	1	7	0.1566	1.945	1.769	1.703	
72	2	7	0.163	1.9498	1.769	1.703	
73	3	6	0.166	1.956	1.769	1.703	
74	3	7	0.1763	1.968	1.769	1.703	
75	3	8	0.1732	1.973	1.77	1.703	
76	2	8	0.1856	1.978	1.771	1.703	

Steps	Location of	of elements		Stre	ss (GPa)	
77	Row	Column	Matrix	Left fiber	Centre fiber	Right fiber
78	1	8	0.1923	1.985	1.774	1.703
79	2	9	0.1971	1.988	1.775	1.703
80	1	9	0.1878	1.991	1.776	1.703
81	3	10	0.1988	1.993	1.783	1.703
82	2	10	0.2051	1.995	1.788	1.703
83	1	10	0.1810	1.997	1.790	1.703

The number of steps which is given in above table is divided into 5 groups. The details explanations of each group is given below.

Group 1: step 1 to step 25, it is noted that Matrix failure is concentrated close to left fiber and the left fiber stress increases gradually. The matrix failure simulation results for step 1 to 25, is shown in figure 3.30.

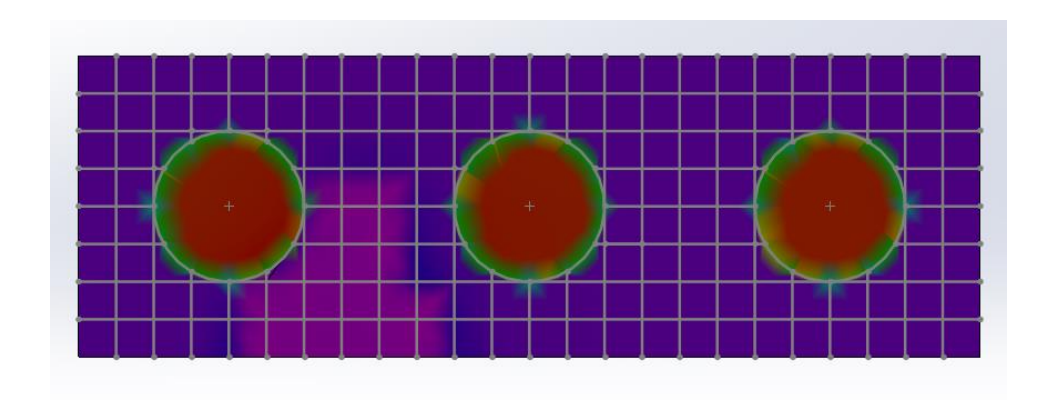


Fig 3.30. after 25 steps, damaged composites

Group 2: step 26 to 35, during these steps, the elements between left and central fiber is completely damage. But the avg. stress acting on composites continued to distribute on left and central fiber, providing the stable condition in composites. The matrix failure simulation results for step 26 to 35, is shown in figure 3.31.

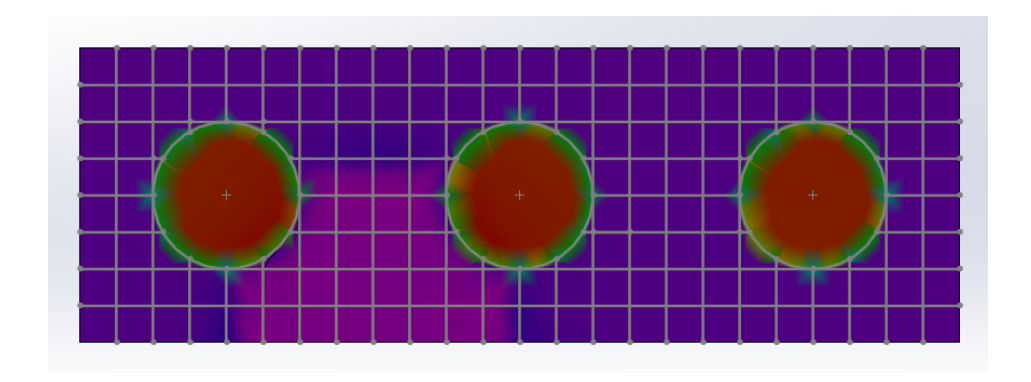


Fig 3.31. after 35 steps, damaged composites

Group 3: step 35 to step 72, during these steps, matrix failure is concentered around left fiber and stress of left fiber is increased while the stress of central fiber remains constant. The matrix failure simulation results for step 35 to 72, is shown in figure 3.32.

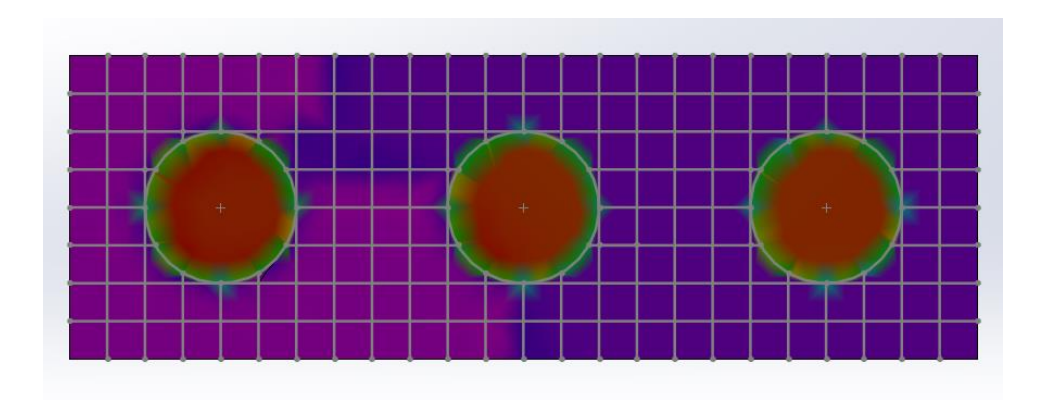
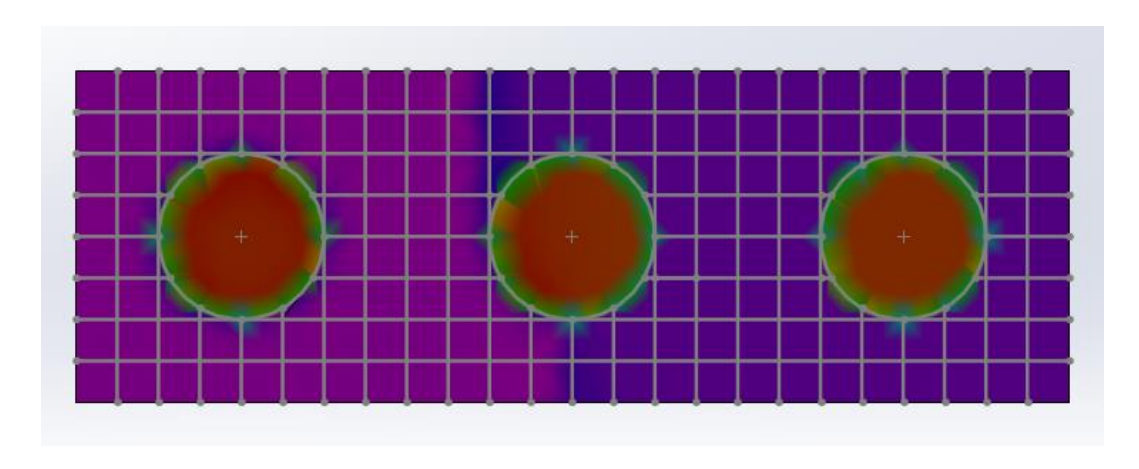


Figure 3.32. after 72 steps, damaged composites

Group 4: step 73 to step 83, during these steps, matrix around left fiber is completely damaged and the stress of left fibers almost reached to the failure stress of glass fiber materials. The matrix damage continues to happen on central fiber region. The matrix failure simulation results for step 73 to 82, is shown in figure 3.33.



Group 5: Step 84, on this step, the matrix failure moves to on central fiber direction and the stress of left fibers reached to the failure stress of glass fiber materials and the left fiber is completely failed. The failure stress of glass fiber materials is 2 GPa and the stress on left fiber exceed 2 GPa Therefore, left fiber fails. The matrix failure and fiber failure simulation are shown below figure 3.34.

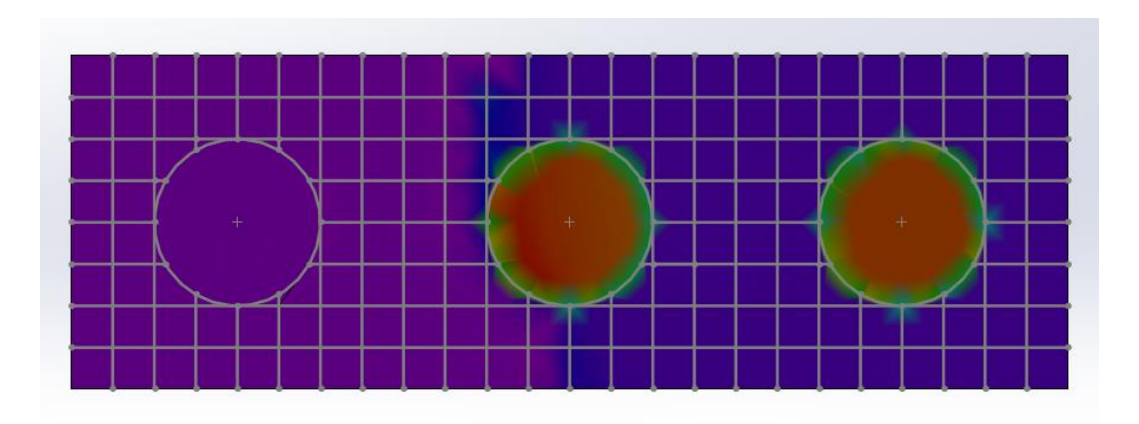


Fig. 3.34. after 84 steps where left fiber and matrix around left fiber are totally failed

The graph below (figure 3.35) shows the result of stress vs all 83 steps performed by applying damage to the individual elements in matrix. According to our assumption, the graph should be in increasing order, but here the graph is increasing but at some point, it shows decreasing results. This can be since we considered average stress for each particular element, but at that elements there will be some points where stress will be very less, or stress will be very high. Also, one of the reasons of this can be, the elements which are close to fiber have large amount of stress concentration because fiber has very high allowable failure stress than matrix. Also, the results can be influence by the inter-laminar failure in matrix. Although there is some inaccuracy in the plot, but the results obtain are quite satisfactory with our assumption.

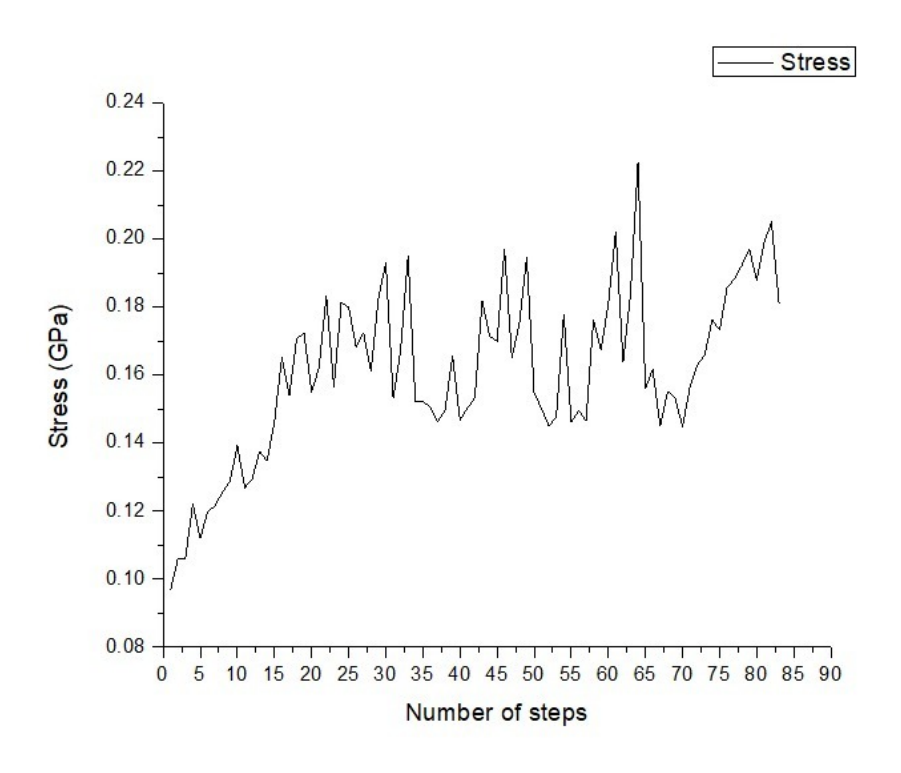


Figure 3.35. the stress distribution for each 83 matrix elements, step by step

The stress distribution in fiber is show in the form of graph (Figure 3.36). From the graph, it can be noted that, the maximum stress is acting on left fiber and the magnitude of that stress is close to 2 GPa. The stress distribution in the center fiber is increases gradually but after some instances it becomes constant. The reason for the constant curve for the middle fiber is that, all the stress due to the damage is transferred to the left fiber. So, there is a sharp increase in the stress curve for the left fiber and after some point of time the left fiber will eventually come to fracture. The stress distribution for the right fiber is constant because all the stress distribution on the composites happen only between left fiber and center fiber. The result would have been perfectly opposite if we would have selected the 1st split elements for damage between right fiber and middle fiber.

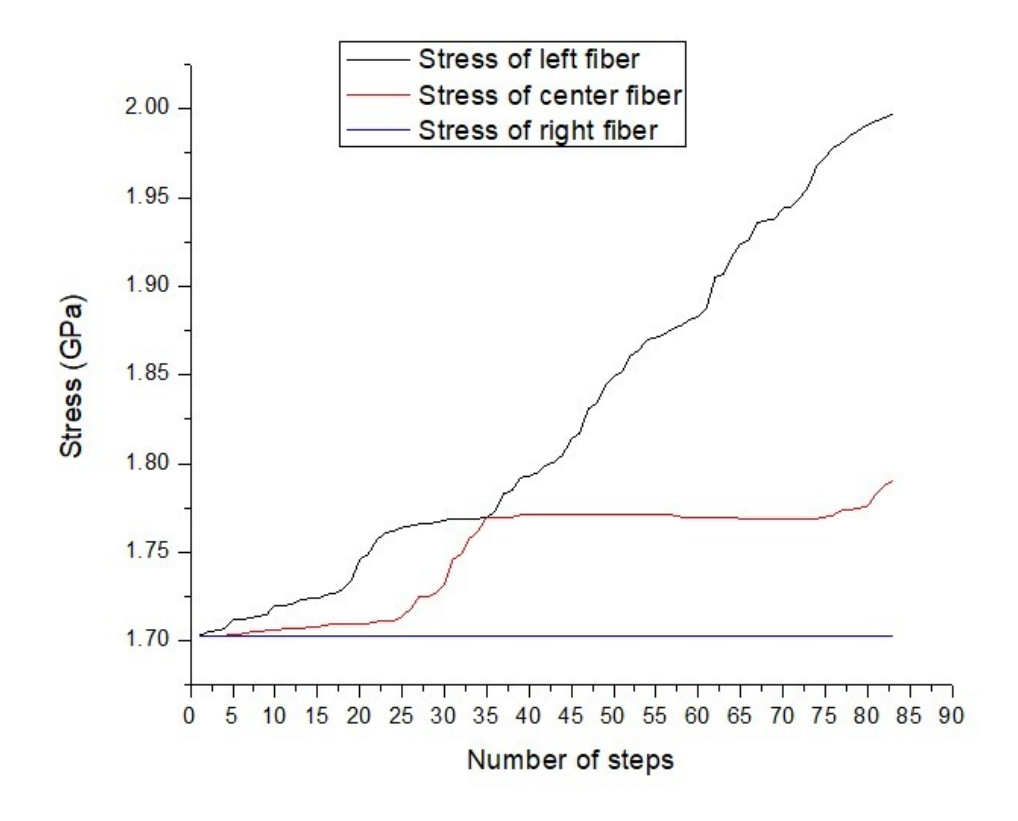


Figure 3.36. the stress of all 3 fibers (left, center and right)

The static simulation for matrix failure done for model 1 using Solid works analysis. After getting results from model 1, we have analyzed that matrix failure occurs first followed by fiber failure. Just for the sake of parametric analysis, in model 2, we will reduce the diameter of the fiber from 0.25 mm to 0.125 mm (half the diameter) and will repeat the same simulation in solid works. As the diameter changes, the fiber volume fraction of composite material will change as well. By doing same simulations on model 2, we will analysis the effect of fiber volume fraction on stress and strain while matrix occurs failure first.

3.2.2. The structure of model 2

As said before, the structure of model 2 is same as model 1, only changed in diameter of all 3 fibers, instead of 0.25 mm diameter in model 1, here obtained 0.125 mm diameter for model 2. All assembly conditions, boundary conditions for simulations and value of mesh, displacement all are same as model 1. Here, also using split features for obtained same simulation in model 1. The properties of materials for fiber and matrix are same as respectively glass fiber and epoxy resin (table 3.1). After changing in diameter, the structure of model 2, is shown figure 3.37.

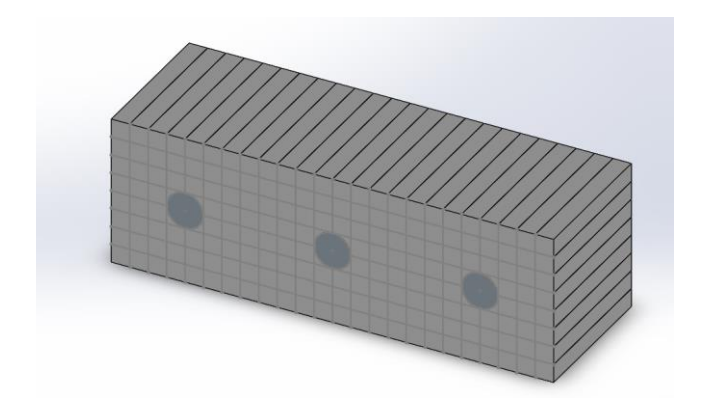


Fig. 3.37. structure of model 2

The post processing operation is carried out in the SOLIDWORKS software after developing the model, discretizing and solving the governing equations by incorporating the appropriate boundary conditions.

Result of simulations

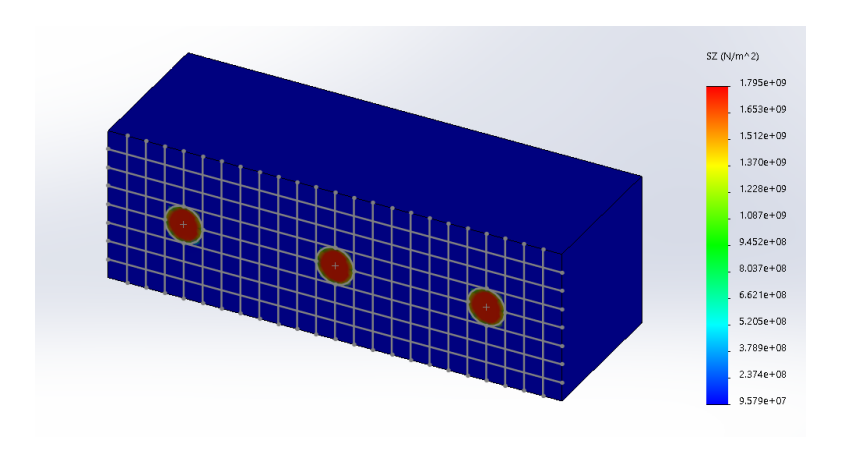


Fig 3.38. stress plot in Z direction

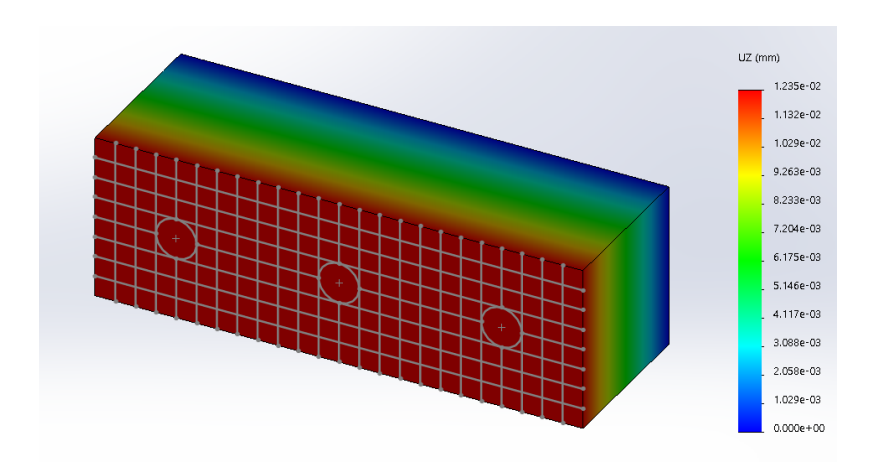


Fig 3.39. displacement plot in Z direction

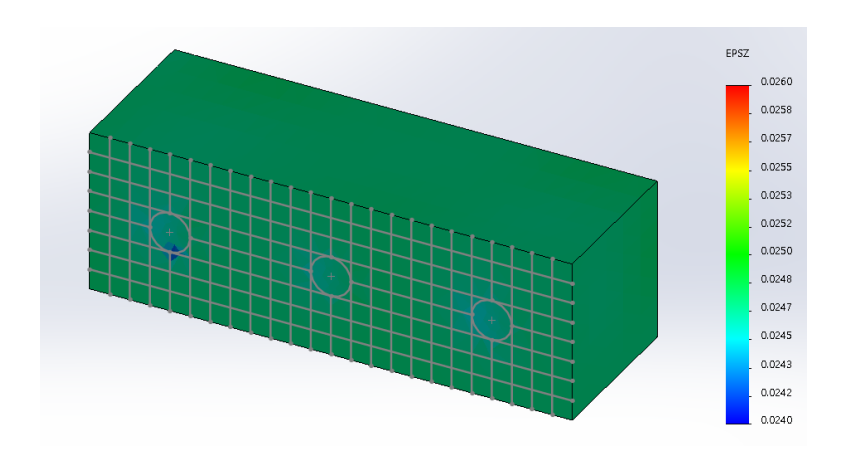


Fig. 3.40. strain plot in Z direction

Again, the matrix failure simulation is carried out by switching off symmetry boundary conditions for the selected elements with maximal average stress. Static simulation is performed, and results are noted. Again, all the steps are repeated, the element with maximal average stress is selected and failure acts on it, the boundary conditions are switched off for that element and matrix failure simulation is performed. This all steps are repeated until composites fails. It is noted from the results, that composites fail after performing 47 steps by selecting 47 individual split elements one by one. The matrix failure simulation for all 47 steps, the stress of matrix and the stress of left, center and right fiber, are given below table 3.4.

Table 3.4

	Location of Elements Stress (GPa)					
Steps	Row	Column	Matrix	Left fiber	Centre fiber	Right fiber
1	4	8	0.099	1.754	1.748	1.76
2	4	7	0.1002	1.754	1.748	1.76
3	4	6	0.1636	1.754	1.748	1.76
4	4	5	0.281	1.756	1.749	1.76
5	5	5	0.2983	1.76	1.749	1.76
6	5	6	0.163	1.76	1.749	1.76
7	6	5	0.1604	1.776	1.749	1.76
8	6	4	0.1617	1.779	1.749	1.76

9	6	6	0.1038	1.783	1.749	1.76	
	Location of	of elements		Stress (GPa)			
Steps	Row	Column	Matrix	Left fiber	Centre fiber	Right Fiber	
10	6	7	0.1099	1.796	1.749	1.76	
11	5	7	0.1127	1.798	1.749	1.76	
12	5	8	0.1191	1.822	1.75	1.76	
13	6	8	0.1265	1.829	1.751	1.76	
14	5	9	0.1222	1.836	1.752	1.76	
15	3	7	0.1209	1.838	1.753	1.76	
16	3	6	0.1206	1.841	1.753	1.76	
17	3	5	0.1672	1.857	1.753	1.76	
18	3	4	0.1628	1.865	1.754	1.76	
19	4	4	0.2898	1.867	1.754	1.76	
20	5	4	0.3069	1.868	1.754	1.76	
21	5	3	0.1584	1.868	1.754	1.76	
22	4	3	0.1584	1.869	1.754	1.76	
23	3	8	0.1288	1.869	1.754	1.76	
24	4	9	0.1236	1.878	1.755	1.76	
25	3	9	0.1336	1.883	1.757	1.76	
26	6	9	0.1346	1.888	1.76	1.76	
27	7	7	0.1331	1.893	1.763	1.76	
28	7	8	0.1349	1.895	1.763	1.76	
29	7	6	0.1382	1.901	1.765	1.76	
30	7	9	0.1399	1.914	1.766	1.76	
31	5	10	0.1404	1.918	1.768	1.76	
32	6	10	0.1414	1.919	1.771	1.76	
33	4	10	0.1493	1.923	1.776	1.76	
34	3	10	0.1437	1.927	1.784	1.76	
35	7	10	0.1438	1.93	1.791	1.76	
36	5	11	0.219	1.933	1.796	1.76	
37	4	11	0.2156	1.934	1.807	1.76	
38	6	11	0.1515	1.936	1.832	1.76	
39	7	11	0.1483	1.938	1.853	1.76	
40	8	8	0.1699	1.94	1.863	1.76	

41	8	9	0.1692	1.942	1.864	1.76
	Location o	of elements	Stress (GPa)			
Steps	Row	Column	Matrix	Left fiber	Centre fiber	Right fiber
42	8	7	0.1939	1.948	1.87	1.76
43	8	10	0.2045	1.961	1.876	1.76
45	8	6	0.1953	1.974	1.901	1.76
46	8	5	0.1794	1.991	1.907	1.759
47	7	5	0.1943	1.996	1.908	1.759

The matrix failure simulation for all 47 steps can be divided into 4 groups, in order to explain stress distribution on the composites. The group are as follows.

Group 1: step 1 to 6, during these steps, the matrix failure is concentrated close to left and center fiber. The stress of left and center fiber is increasing gradually, and the stress of right fiber is constant. The matrix failure simulation results for step 1 to 6, is shown in figure 3.41.

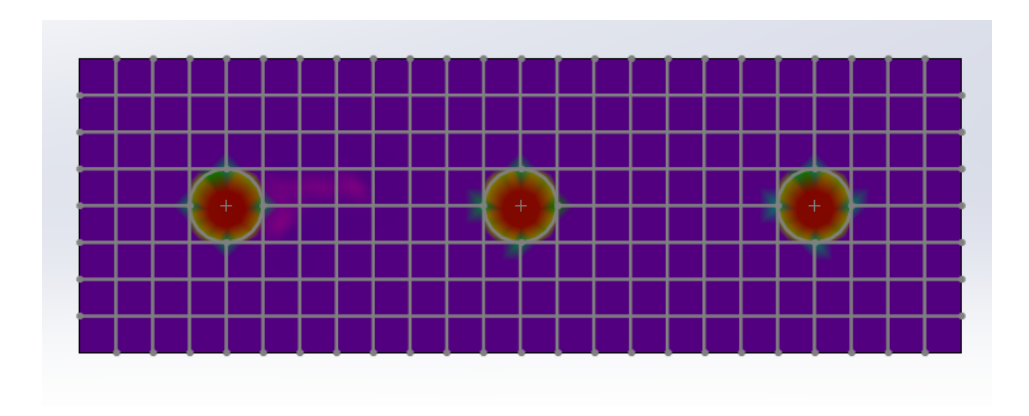


Fig 3.41. after 6 steps, damaged composites

Group 2: step 7 to 25, during these steps, the matrix failure is concentered around left and center fiber and stress of left fiber is increased while the stress of central fiber remains approx. constant. The matrix failure simulation results for step 7 to 25, is shown in figure 3.42.

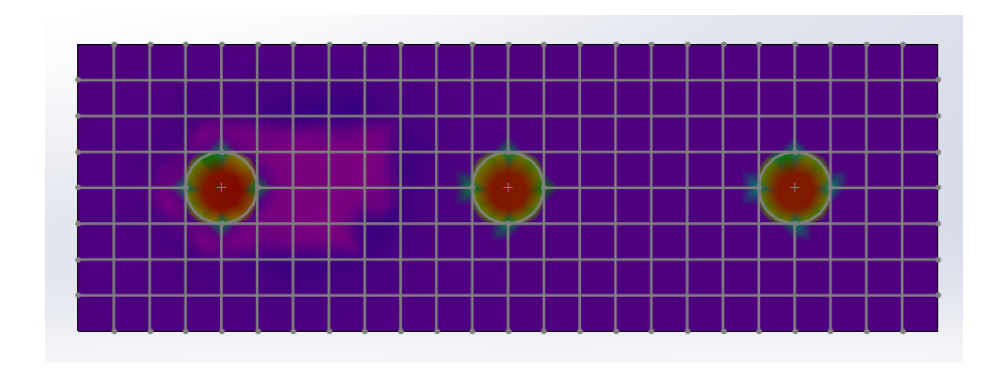


Fig 3.42. after 25 steps, damaged composites

Group 3: step 26 to 47, during these steps, the matrix failure is concentered around left and center fiber and stress of left fiber is increased, and stress of center fiber increased as well as. The stress of left fibers almost reached to the failure stress of glass fiber materials. The matrix failure simulation results for step 26 to 47, is shown in figure 3.43.

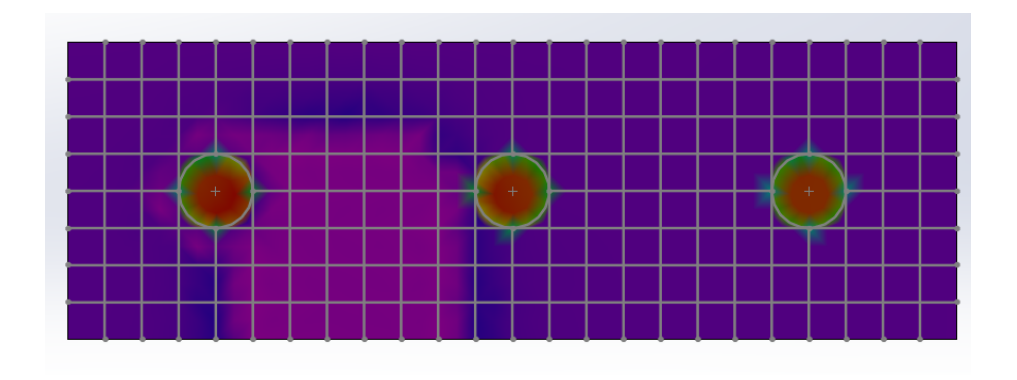


Fig 3.43. after 47 steps, damaged composites

Step 4: Step 48, on this step, the matrix failure happened around left fiber and the stress of left fibers reached to the failure stress of glass fiber materials and the left fiber is completely failed. The failure stress of glass fiber materials is 2 GPa and the stress on left fiber exceed 2 GPa Therefore, left fiber fails. The matrix failure and fiber failure simulation are shown below figure 3.44.

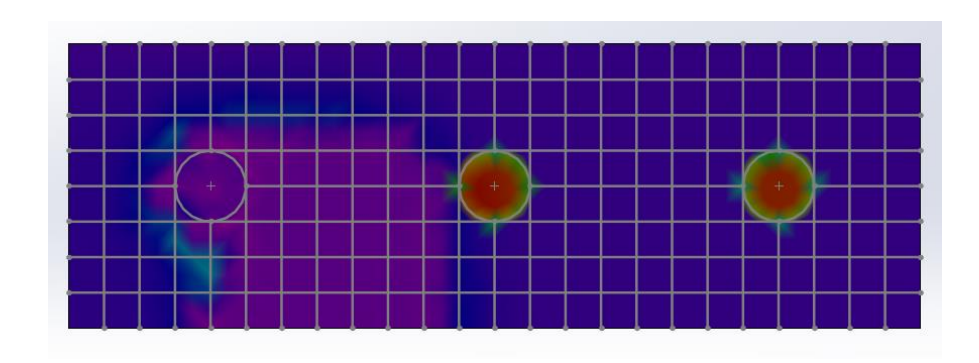


Fig 3.44. after 48 steps, left fiber is failed

The graph below (figure 3.45) shows the result of stress vs all 49 steps performed by applying damage to the individual elements in matrix. According to our assumption, the graph should be in increasing order, but here the graph is increasing but at some point, it shows decreasing results. The reasons behind that already described before in model 1.

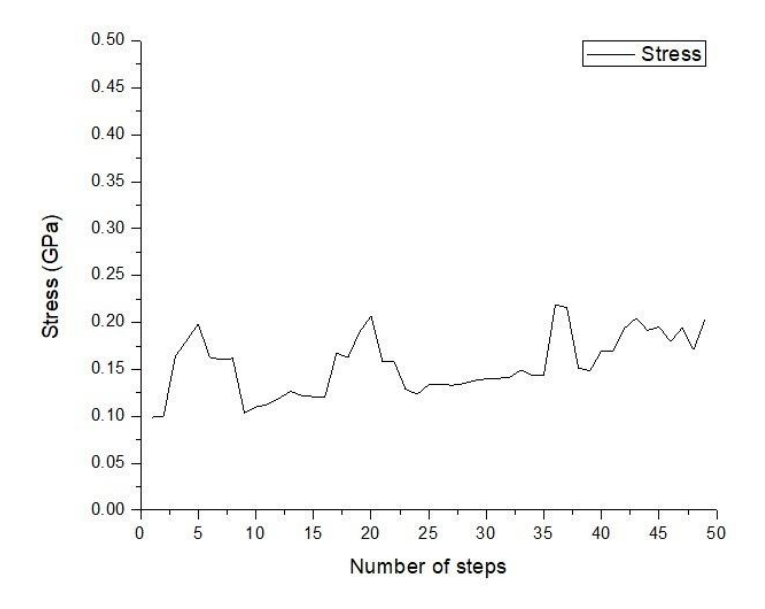


Fig 3.45. stress distribution for each 47 matrix elements

The stress distribution in fiber is show in the form of graph (Figure 3.46). From the graph, it can be noted that, the maximum stress is acting on left fiber and the magnitude of that stress is close to 2 GPa. The stress distribution in the center fiber is constant but after some time it increased gradually. The reason for the constant curve for the middle fiber is that, all the stress due to the damage is transferred to the left fiber and after some steps, stress of center fiber is also taking stress while damage in composites. So, there is a sharp increase in the stress curve for the left fiber and after some point of time the left fiber will eventually come to fracture.



Fig 3.46. stress distribution in fiber, how they distributed stress

3.3. Compare the results

After completing static simulation for both models, created one graph that shows in figure 3.47 From the graph, it can be concluded that, the maximum stress is acting on left fiber, but in both models, the time of fiber failure or steps of fiber failure is different. This can be due to the how fiber volume fraction effects on composites. When fiber volume fraction is higher, the volume of fiber is also high and due to the strength of fiber, fiber become more stronger compare to the lower volume of the fiber in composites. In our cases, the fiber volume fraction for model 1 and model 2 respectively 0.1963 and 0.049 which calculated by theoretical.

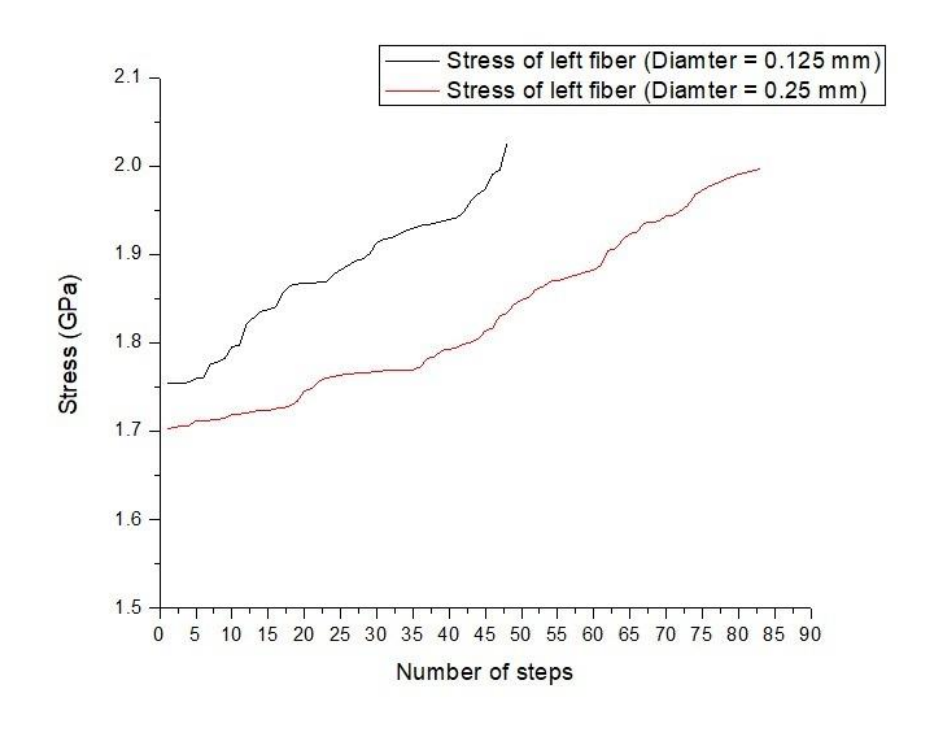


Figure 3.47. the left fiber stress vs step number (for both model)

Conclusions

FEM analysis is performed for composites by applying damage in 1) fiber and 2) matrix. By looking at the result of fiber failure, it can be said that if fiber failure happens first then the stress in composites should be in increasing order, but the result does not satisfactorily coincide with the given assumption. The numerical results for matrix failure show good qualitative and quantitative agreement with the given assumptions. The given FEM analysis is suitable for brittle materials. It is not possible to perform such analysis in ductile material, because this material does not show linear elastic behaviour before failure. When the damage is applied to the matrix, the matrix does not damage completely. At the same time the stresses due to the damage are transferred to the fiber until the fiber fails. This provides additional strength to the composites before it fails. The strength of the composites is directly proportional to the volume fraction of the fiber.

Bibliography

- 1. http://www.scienceclarified.com/Ci-Co/Composite-Materials.html
- 2. D. Hull, T. W. Clyne, An Introduction to Composite Materials (Cambridge Solid State Science Series), 1996.
- 3. Razali, N., M. T. H. Sultan, F. Mustapha, N. Yidris, and M. R. Ishak. "Impact damage on composite structures—a review." The International Journal of Engineering and Science 3, no. 7 (2014): 08-20.
- 4. Ghobadi, A. Common Type of Damages in Composites and Their Inspections. World Journal of Mechanics, 7, 24-33. (2017)
- 5. Ghobadi, Amin. "Common type of damages in composites and their inspections." World Journal of Mechanics 7, no. 2 (2017): 24-33.
- Razali, Noorshazlin, M. T. H. Sultan, and Mohammad Jawaid. Impact damage analysis of hybrid composite materials. In Durability and Life Prediction in Biocomposites, Fibre-Reinforced Composites and Hybrid Composites, pp. 121-132. Woodhead Publishing, 2019.
- 7. Ramesh Talreja, Texas A & M University, Chandra Veer Singh, University of Toronto https://doi.org/10.1017/CBO9781139016063.004
- 8. Harris, B. "Micromechanisms of crack extension in composites." Metal Science 14, no. 8-9 (1980): 351-362.
- 9. https://sci-hub.tw/ https://www.tandfonline.com/doi/abs/10.1179/msc.1980.14.8-9.351
- 10. http://www.ae.iitkgp.ac.in/ebooks/
- 11. Giurgiutiu, Victor. "Predictive simulation of guide wave structural health monitoring in metallic and composite structures." In Proceedings of the 9th European Workshop on Structural Health Monitoring EWSHM. 2018.
- 12. http://home.iitk.ac.in/~mohite/Composite_introduction.pdf
- 13. http://medieval2.heavengames.com/
- 14. https://www.rsc.org/Education/Teachers/Resources/Inspirational/resources/4.3.1.pdf
- 15. Ha, Sung Kyu, Kyo Kook Jin, and Yuanchen Huang. "Micro-mechanics of failure (MMF) for continuous fiber reinforced composites." Journal of Composite Materials 42, no. 18 (2008): 1873-1895.

- 16. https://www.cambridge.org/core/books/damage-and-failure-of-composite materials/damage-in-composite materials/79913CFC3E07B24C0A9CBBECC0B96510#fndtn-references
- 17. Jeongguk, K., Liaw, P.K. and Wang, H. (2003) The NDE Analysis of Tension Behavior in Nicalon/SiC Ceramic Matrix Composites. Journal of the Minerals, 55, 1-13.
- 18. Wikipedia. https://en.wikipedia.org/wiki/Delamination
- 19. Khoshravan, M.R. and Khalili, A. (2015) Modeling of Failure by Delamination in Curved Composite Beams. Applied Mathematics in Engineering, Management and Technology, 3, 31-42.
- 20. Hull, D. and Clyne, T.W. (1996) An Introduction to Composite Materials. Cambridge University Press, Cambridge. https://doi.org/10.1017/CBO9781139170130
- 21. Muñoz, E. and García-Manrique, J.A. (2015) Water Absorption Behaviour and Its Effect on the Mechanical Properties of Flax Fibre Reinforced Bioepoxy Composites. International Journal of Polymer Science, 2015, 1-10.
- 22. Arif, M.F., Meraghni, F., Chemisky, Y., Despringre, N. and Robert, G. (2014) In Situ Damage Mechanisms Investigation of PA66/GF30 Composite: Effect of Relative Humidity. Composites Part B: Engineering, 58, 487-495. https://doi.org/10.1016/j.compositesb.2013.11.001
- 23. Khoshravan, M.R., Samaei, M. and Khalili, A. (2010) Numerical Analysis of the Situation of Holes for Decreasing the Stress Concentration in Composite Plates in Bolted Joints. 9th Annual Iranian Aerospace Society Conference, Tehran, 11-13 A. Ghobadi 31 May 2010
- 24. Khoshravan, M.R., Samaei, M. and Paykani, A. (2011) Numerical Investigation on the Position of Holes for Reducing Stress Concentration in Composite Plates with Bolted and Riveted Joints. Theoretical and Applied Mechanics Letters, 1, Article ID: 041005.
- 25. https://doi.org/10.1063/2.1104105 [17] Masoomi, M. (2014) Numerical Modeling of Thermal Effects during Selective Laser Melting. 10th Mississippi State Conference on Differential Equations and Computational Simulations, Starkville, 23-25 October 2014.
- 26. Masoomi, M., Gao, X., Thompson, S.M., Shamsaei, N., Bian, L. and Elwany, A. (2015) Modeling, Simulation and Experimental Validation of Heat Transfer during Selective Laser Melting. ASME 2015 International Mechanical Engineering Congress

- and Exposition, Houston, 13-19 November 2015, V02AT02A007. https://doi.org/10.1115/imece2015-52165
- 27. Gharghabi, P., Lee, J., Mazzola, M.S. and Lacy, T.E. (2016) Development of an Experimental Setup to Analyze Carbon/Epoxy Composite Subjected to Current Impulses. Proceedings of American Society for Composites Annual Technical Conference, Williamsburg, 19-22 September 2016.
- 28. Peyman, D.-B., Pedram, G. and Kaveh, N. (2011) Impact of Metal Thickness and Field Shaper on the Time-Varying Processes during Impulse Electromagnetic Forming in Tubular Geometries. Journal of the Korean Physical Society, 59, 3560.
- 29. https://doi.org/10.3938/jkps.59.3560
- 30. Peyman, D.B., Pedram, G. and Kaveh, N. (2011) Dynamic Analysis of a Fast-Acting Circuit Breaker (Thompson) Drive Mechanism. Journal of the Korean Physical Society, 59, 3547-3554. https://doi.org/10.3938/jkps.59.3547
- 31. N.J. Hoff, Innovation in Aircraft Structures-Fifty years Ago and Today, AIAA Paper No. 84-0840,1984.
- 32. R.J. Schliekelmann, A Soft and Hard Future A Look into Past and Future Developments of Structural Materials, AIAA International Annual Meeting on Global Technology 2000, Baltimore, 1980.
- 33. M. Lee (Ed.), International Encyclopedia of Composites, Vols.1-6, VCH Publishers, New York 1990-1991.
- 34. J.W. Weeton, D.M. Peters and K.L. Thomas (Eds.) Engineer's Guide to Composite Materials, American Society of Metals, Metals Park, Ohio,1987.
- 35. https://file.scirp.org/pdf/WJM_201702221
- 36. https://www.scirp.org/journal/PaperInfor
- 37. Yildirim, Mehmet Nuri, Burhanettin Uysal, Ayhan Ozcifci, and Ahmet H. Ertas. "Determination of fatigue and static strength of Scots pine and Beech wood." *Wood research* 60, no. 4 (2015): 679-686.
- 38. Miyano, Y., Nakata, M. and Sekine, N. (2005). Accelerated Testing for Long-Term Durability of FRP Laminates for Marine Use, Journal of Composite Materials, 39: 5–20.
- 39. Miyano, Y., Nakada, M. and Cai, H. (2008). Formulation of Long-Term Creep and Fatigue Strengths of Polymer Composites based on Accelerated Testing Methodology, Journal of Composite Materials (In print).

- 40. Jin, K.K., Huang, Y., Lee, Y.H. and Ha, S.K. (2008). Distribution of Micro Stresses and Interfacial Tractions in Unidirectional Composites, Journal of Composite Materials (In print).
- 41. Altenbach, H. and Tushtev, K. (2001). A New Static Failure Criterion for Isotropic Polymers, Mechanics of Composite Materials, 37(5–6): 475–482.
- 42. Bowden, P.B. and Jukes, J.A. (1972). The Plastic Flow of Isotropic Polymers, Journal of Material Science, 7: 52–63.
- 43. Raghava, R.S., Caddell, R.M. and Yeh, G.S.Y. (1973). The Macroscopic Yield Behavior of Polymers, Journal of Material Science, 8: 225–232.
- 44. Bauwens, J.C. (1970). Yield Condition and Propagation of Lu" ders' Lines in Tension-Torsion Experiments on Poly (Vinyl Chloride), Journal of Polymer Science Part A-2: Polymer Physics, 8(6): 893–901.
- 45. Sato, Mio, Sakie Shirai, Jun Koyanagi, Yuichi Ishida, and Yasuo Kogo. "Numerical simulation for strain rate and temperature dependence of transverse tensile failure of unidirectional carbon fiber-reinforced plastics." Journal of Composite Materials 53, no. 28-30 (2019): 4305-4312.
- 46. Carrera, E., I. Kaleel, and M. Petrolo. "Numerical Simulation of Failure in Fiber Reinforced Composites." (2019).
- 47. Qin, Tianliang, Libin Zhao, Jifeng Xu, Fengrui Liu, and Jianyu Zhang. "Model of CEL for 3D elements in PDMs of unidirectional composite structures." Computer Modeling in Engineering & Sciences 118, no. 1 (2019): 157-176.
- 48. Koyanagi, Jun, Yukihiro Sato, Toshiki Sasayama, Tomonaga Okabe, and Satoru Yoneyama. "Numerical simulation of strain-rate dependent transition of transverse tensile failure mode in fiber-reinforced composites." Composites Part A: Applied Science and Manufacturing 56 (2014): 136-142.
- 49. Koyanagi, Jun, Akinori Yoshimura, Hiroyuki Kawada, and Yuichiro Aoki. "A numerical simulation of time-dependent interface failure under shear and compressive loads in single-fiber composites." Applied Composite Materials 17, no. 1 (2010): 31-41.
- 50. Laš, Vladislav, and Robert Zemčík. "Progressive damage of unidirectional composite panels." Journal of Composite Materials 42, no. 1 (2008): 25-44.
- 51. https://www.innova-systems.co.uk/use-split-feature-solidworks/

- 52. https://hawkridgesys.com/blog/solidworks-trim-surface-split-split-line-whats-difference
- 53. Mechanics of Fibrous Composites, CT Herakovich, Wiley 1998.